Journal of Plant Growth Regulation (2022) 41:2930–2948
https://doi.org/10.1007/s00344-021-10485-1

Interactive Effects of Abiotic Stress and Elevated CO_2 on Physio-Chemical and Photosynthetic Responses in *Suaeda* Species

Md Intesaful Haque[1] · Shahrukh A. Siddiqui[1] · B. Jha[1] · Mangal S. Rathore[1]

Received: 21 January 2021 / Accepted: 26 August 2021 / Published online: 4 September 2021

Abstract

Suaeda fruticosa and *S. monoica* are important halophytes for ecological rehabilitation of saline lands. We report differential physio-chemical, photosynthetic, and chlorophyll fluorescence responses in these halophytes under 100 mM sodium chloride (NaCl), 50% strength (16.25 ppt) of seawater (SW)-imposed salinity, and 10% polyethylene glycol 6000 imposed osmotic stress at 380 (ambient) and 1200 (elevated) µmol mol^{-1} CO_2 concentrations. SW salinity enhanced the growth in both species; however, compared with *S. fruticosa,* the *S. monoica* exhibited comparatively better growth and biomass accumulation under saline conditions at elevated CO_2. Results demonstrated better photosynthetic performances of *S. monoica* under stress conditions at both levels of CO_2, and this resulted in higher accumulation of carbon, nitrogen, sugar, and starch contents. *S. monoica* exhibited improved antenna size, electron transfer at PSII donor side, and efficient working of photosynthetic machinery at elevated CO_2, which might be due to efficient upstream utilization of reducing power to fix the CO_2. The $\delta^{13}C$ results supported the operation of C_4 CO_2 fixation in *S. monoica* and C_3 or intermediate pathway of CO_2 fixation in *S. fruticosa*. Lower accumulation of reactive oxygen species, reduced membrane damage, lowered solute potential, and higher accumulation of proline and polyphenol contents indicated elevated CO_2-induced abiotic stress tolerance in *Suaeda*. Higher activity of antioxidant enzymes in both species at both levels of CO_2 help plants to combat the oxidative stress. Upregulation of *NADP-dependent malic enzyme* and *NADP-dependent malate dehydrogenase* genes indicated their role in abiotic stress tolerance as well as photosynthetic carbon (C) sequestration. Operation of C_4 type CO_2 fixation in *S. monoica* and an intermediate CO_2 fixation in *S. fruticosa* could be the possible reason for the superior photosynthetic efficiency of *S. monoica* under stress conditions at elevated CO_2.

Keywords CO_2-concentrating mechanism · C-sequestration · Halophytes · Photosynthetic efficiency and *Suaeda*

Introduction

Environmental stresses are the major threats to plant productivity (Ahammed et al. 2020a). Among various abiotic stresses, salinity and osmotic stress are the most common stresses and inter-related with each other in their physiological responses (Zhang et al. 2010). Salinity and osmotic stress negatively affect the plant development and result in lower productivity (Ahammed et al. 2018). Halophytes acquired excellent tolerance ability against salt and osmotic stress, and besides saline land reclamation, these can be exploited as cash crops and biomass producing crops (Rathore et al. 2016). Photosynthesis in plants is one of the major processes adversely affected by salinity and osmotic stress through reduction in CO_2 fixation. CO_2 is the key input for photosynthesis; therefore, varying CO_2 concentrations have diverse effects on crop productivity (Sage and Coleman

Handling editor: Golam jalal Ahammed.

✉ Mangal S. Rathore
mangalrathore@csmcri.res.in; mangalrathore@gmail.com

Md Intesaful Haque
intesafulhaque@gmail.com

Shahrukh A. Siddiqui
shahrukh2990@gmail.com

B. Jha
bjha@gmail.com

[1] Division of Applied Phycology and Biotechnology, Council of Scientific and Industrial Research—Central Salt and Marine Chemicals Research Institute (CSIR-CSMCRI), G.B. Marg, Bhavnagar, Gujarat 364002, India

2001; Ahammed et al. 2020b). The global climatic scenario is continuously changing and it is assumed that the level of CO_2 will reach 1000 µmol mol^{-1} air by the end of this century, which will directly affect the photosynthesis (Li et al. 2019). Thus, the salinity and osmotic stress through reducing the soil fertility and the elevated CO_2 (eCO_2) with various effects on photosynthesis will become the major factors in determining the global crop productivity. One of the solutions under such conditions is the development of abiotic stress-tolerant crop having higher carbon (C) sequestration ability; however, it looks like a difficult solution. Another most promising approach is the use of halophytes that grow naturally under saline conditions and have better photosynthetic yield under abiotic stress conditions. Several halophytes find role as food, fodder, and in coastal protection, thus, possess potential for salty-land/wasteland reclamation (Giessler et al. 2009). The eCO_2 up to certain levels improves the plant growth and productivity by increasing the CO_2 fixation, and this enhances the tolerance against various abiotic stresses (Ainsworth and Rogers 2007; Pan et al. 2018). Thus, studying the effect of eCO_2 in halophytes under abiotic conditions would be interesting and help to understand the mechanism involved in plant responses under interactive environment of eCO_2 and abiotic stress.

The eCO_2 increases the C assimilation, reduces stomatal conductance and N concentrations, and increases water-use efficiency (Ainsworth and Rogers 2007; Ellsworth et al. 2004; Morgan et al. 2011). The higher supply of CO_2 in plants imparts certain level of stress tolerance through elevated photosynthesis (Zhang et al. 2020a, b). The eCO_2 improves photosynthesis with strong stimulatory effect in C_3 plants like *Sorghum bicolor* and *Zea mays*, whereas it has no effect on photosynthesis in C_4 plants like *Andropogon gerardii*, *Schizachyrium scoparium,* and *Sorghastrum nutans* (Long et al. 2004). In *Amaranthus* and sugarcane, eCO_2 alleviated the negative impact of mild water stress and had no effect under severe water stress (Ghannoum 2009). The improved survival of *Aster tripolium* L. at eCO_2 under sodium chloride (NaCl) stress showed the positive impact of interactions between salinity and eCO_2 on growth, photosynthesis, water relations, and chemical compositions in halophytes (Geissler et al. 2009, 2010). The higher CO_2 leads to better water balance, reduction in stomatal conductance (g_s), and improved osmotic potential in plants under saline stress; however, no significant biomass variations were recorded in *Salicornia ramosissima,* and this was attributed to the investment of higher energy for salinity stress defense mechanisms (Pérez-Romero et al. 2018). Atmospheric eCO_2 enhanced the photosynthesis in C_3 (*Chenopodium quinoa*) and C_4 (*Atriplex nummularia*) halophyte; however, *A. nummularia* distinctly showed a higher level of salt resistance as compared to *C. quinoa* (Geissler et al. 2015). The CO_2-concentrating mechanism in C_4 plants supports their better survival under stress conditions through concentrating the CO_2 around Rubisco, which minimizes the oxygenase activity and the resultant loss of carbon through photorespiration.

Suaeda fruticosa (L.) Forssk and *S. monoica* Forssk. ex J. F. Gmel are the two important halophytes exhibiting luxuriant growth under abiotic stress and possess potential of ecological rehabilitation of saline land. *Suaeda* genus possesses both C_3 and C_4 photosynthetic C fixation pathways with and without typical *Kranz* anatomy (Shomer-Ilan et al. 1975). The presence of *Kranz* anatomy was reported as an essential criterion for C_4 photosynthetic operation; however, numerous literature reports demonstrated the functioning of C_4 pathway in single-cell system or without typical *Kranz* anatomy (Park et al. 2009; Koteyeva et al. 2011; Shomer-Ilan et al. 1975). The C_4 mode of CO_2 fixation is comparatively efficient and advantageous over the C_3 mode under hot, dry, and saline habitats. Salinity and osmotic stress primarily reduce the stomatal conductance and interfere with photosynthetic CO_2-diffusion. The cost of photorespiration has been reported as the driving force behind the evolution of C_4 photosynthesis (Sage 2004; Gowik and Westhoff 2011). Water stress severely affects C_4 photosynthesis by reducing the intercellular CO_2 concentrations; however, initially, the responses are not very harmful as the C_4 pathway is capable of supplying CO_2 through PEPC-medicated re-fixation of respiratory CO_2 before escaping the bundle sheath. The abiotic stresses increase photorespiration as an adaptive response to maintain the availability of photosynthetic assimilates (Khatri and Rathore 2019).

The increasing atmospheric CO_2, temperature, drought, and salinity strongly influence plant growth, productivity, habitat fragmentation, and C balance in a terrestrial ecosystem. The drought/osmotic and saline conditions are thought to suppress the photosynthetic activity in plants, and at the same time, eCO_2 is expected to enhance the photosynthetic activity. Both C_3 and C_4 halophytes are well adapted to stress conditions; therefore, it would be interesting to evaluate the performance of *S. fruticosa* and *S. monoica* under abiotic stress at eCO_2. Further, despite the progress in understanding the mechanism of plant responses to the eCO_2, very few attempts have been made to study the effect of eCO_2 in halophytes. Therefore, the focus of present study was to evaluate the interactive effect of salinity (NaCl and SW) and osmotic (polyethylene glycol-6000; PEG) stress with eCO_2 (1200 µmol mol^{-1}) on *S. fruticosa* and *S. monoica* to understand the physiological and photosynthetic responses involved in their survival during harsh conditions. The results would provide insights in understanding the mechanism involved in regulation of their growth, development, and biomass production in halophytes under abiotic stress conditions at eCO_2. The results would help to choose the suitable species for biomass production through vegetation restoration in the degraded land.

Material and Methods

Plant Growth and Stress Treatment

Seeds of *S. fruticosa* and *S. monoica* were collected from mature plants growing along Bhavnagar seacoast (Gujarat, INDIA). Seeds were sterilized and germinated on sterile garden soil in 500 ml capacity plastic pots (each pot contained 350 g soil and made porous to avoid waterlogging) at 30 ± 2 °C under diffused light conditions. The plants were irrigated with tap water. 7 days (d) old seedlings were transferred at 26 ± 1 °C for 12 h per day (hd^{-1}) photoperiod of 1000 µmol m^{-2} s^{-1} photosynthetic photon flux density (PPFD) in a plant growth chamber (PGC-105, Percival, USA). The 6 weeks old and uniform plantlets were incubated at 380 [ambient (aCO_2)] and 1200 (eCO_2) µmol mol^{-1} CO_2 concentrations in separate growth chambers and acclimatized for a week. In our previous observationks, at 1200 µmol mol^{-1} of CO_2 in both species exhibited the highest photosynthesis rate (P_N); therefore, this concentration was considered as eCO_2. The plants (both at aCO_2 and eCO_2) were regularly irrigated with aqueous solution of 100 mM NaCl, 50% strength of SW salinity (16.25 ppt), and 10% PEG for 7 d to impose the salinity and osmotic stress. Tap water was used to irrigate the control set of plants. Fig. S1 depicted detailed experimental design. After 7 d, the photosynthetic gas exchange and chlorophyll fluorescence performances were recorded. The samples (from control and stress-treated plants) were harvested and stored at − 80 °C for subsequent physiochemical analysis. A separate set of the experiment continued for 15 d to analyze the growth and morphological symptoms in plants.

Histological Observations, Determination of Plant Growth, and Water Contents

Fresh leaf samples of both *S. fruticosa* and *S. monoica* growing under greenhouse conditions (27 ± 2 °C temperature, 50–60% relative humidity, and ambient light) were cut transversely. The field emission scanning electron microscope (SEM; JSM-7100F, JEOL USA) using Cryo-GATAN facility was used to document the anatomical features. Morphological symptoms and growth in plants were recorded on 0th, 7th, and 15th d of stress treatments at both levels of CO_2. The fresh/dry weight biomass (FW/DW) and root growth were recorded after 15th d of stress treatments. Uniform plant tissues of approximately 100 mg (FW) from apical portions of control and stressed plants were dried at 80 °C for 48 h in a hot air oven, and DW was recorded. The water content (WC; ml g^{-1} FW) was calculated as (FW − DW/FW of sample) and subsequently converted as % of FW.

Elemental and $\delta^{13}C$ Analysis in *Suaeda* Species

Fresh leaf samples from plants growing in natural habitat were harvested, dried, and powdered. The C and N elements were analyzed using an elemental analyzer (vario MICRO cube, Elementar, Germany). The leaf samples were also analyzed for C and its stable isotope ratios ($\delta^{13}C$) using elemental analyzer (vario MICRO cube, Elementar, Germany)—isotope ratio mass spectrometry (IsoPrime100, Isoprime Ltd., UK) following Chaudhary et al. (2018). The system was calibrated using international standards from the International Atomic Energy Agency. The Pee Dee Belemnite (PBD) was used as standard C and isotopic signals were expressed as δ notation as $\delta^{13}C\ ‰ = [(R_{sample} - R_{standard})/R_{standard}] \times 10^3$; where R = ratio ^{13}C:^{12}C of the samples.

Determination of Ion Contents and Energy-Dispersive X-Ray Analysis

Oven-dried and pre-weighed samples were acid [perchloric acid and nitric acid solution (3:1 v/v)] digested and heated to dryness. The residue was dissolved in deionized water, and the ion contents (Na^+ and K^+) were estimated by inductive coupled plasma optical emission spectrometer (Optima2000DV, PerkinElmer, Germany). Alternatively, energy-dispersive X-ray (EDX) mapping was performed for Na^+ and K^+ contents. For EDX analysis, leaf was cut into thin sections and mounted on a stub. Samples were loaded in a scanning electron microscope (SEM; JSM-7100F, JEOL USA) equipped with a quantitative EDX machine. The vacuum was applied to the samples for 30 min, and, subsequently, the mapping was performed following the instructions provided in the machine manual.

Determination of Electrolyte Leakage and MDA Content

The fresh leaves (uniform) harvested from stressed and unstressed *Suaeda* plants were washed with deionized water and immersed in 10 ml deionized water in a set of closed vials. These were incubated at 26 °C on a gyratory shaker for 24 h. The electrical conductivity (EC) of the solution (EC_1) was measured using a conductivity meter (SevenEasy, Mettler Toledo AG 8603, Switzerland). These samples were autoclaved at 121 °C for 15 min, cooled up to 26 °C, and EC (EC_2) was measured. The electrolyte leakage (%EL) was calculated as $(EC_1/EC_2) \times 100$.

The lipid peroxidation was determined by estimating the malondialdehyde (MDA) concentration (nmol g^{-1} FW) following Hodges et al. (1999). The samples were extracted

with 0.1% trichloroacetic acid (TCA), and 0.2 ml extract was reacted with 0.8 ml of thiobarbituric acid (TBA) reagent (0.5% TBA in 20% TCA) and subsequently boiled at 95 °C for 30 min. Samples were ice cooled and centrifuged at 10,000 × *g* for 5 min, and absorbance was read at 440, 532, and 600 nm.

Determination of ROS Accumulation and Activity of Antioxidant Enzymes

Accumulations of reactive oxygen species (ROS) namely hydrogen peroxide (H_2O_2) and superoxide (O_2^-) were determined in vivo in fresh leaf samples from apical portion of the shoots. Accumulation of H_2O_2 was detected by immersing the samples in 3,3-diaminobenzidine (DAB) solution (1 mg ml^{-1} in 10 mM phosphate buffer; pH 3.8) at room temperature (RT) for 12 h in dark, thereafter exposing the samples to intense light until the brown spots showing accumulation of H_2O_2 appeared. Accumulation of O_2^- was detected by immersing the fresh samples in nitro-blue tetrazolium (NBT) solution (1 mg ml^{-1} in 10 mM phosphate buffer; pH 7.8) at RT for 6 h, thereafter, exposing to high irradiance for 12 h until the blue spots showing accumulation of O_2^- appeared. Before documentation, the chlorophyll contents were bleached by ethanol washing.

The samples were ground in liquid nitrogen, and the total protein was extracted in protein extraction buffer [Tris buffer: 50 mM (pH 7.0), 1 mM EDTA, 0.05% (w/v) triton x-100, and 5% (w/v) polyvinylpolypyrrolidone]. Total protein in the extract was determined following Bradford method (Bradford 1976). This extract was used for determination of the activity of catalase (CAT), superoxide dismutase (SOD), and guaiacol peroxidase (GPOX). The SOD activity was determined by monitoring the inhibition of nitro-blue tetrazolium (NBT) reduction following Beyer and Fridovich (1987). The NBT reduction was recorded at 560 nm, and the amount of enzyme required for 50% inhibition of NBT was considered as one-unit activity. The CAT activity was determined by monitoring the disappearance of H_2O_2 (Miyagawa et al. 2000) and taking 43.6 M^{-1} cm^{-1} as an extinction coefficient (Δe) at 240 nm (Patterson et al. 1984). The GPOX activity was determined following Jebara et al. (2005) by reading absorbance at 470 nm and considering 26.6 mM^{-1} cm^{-1} as Δe.

Determination of Solute Potential and Photosynthetic Pigments

Fresh leaf tissues were frozen in liquid nitrogen, thawed, and centrifuged for 10 min at 10,000 × *g* to extract the sap. The ionic strength of the sap was measured using Vapro Pressure Osmometer (model-5600; Wescor, Logan UT, USA). Solute potential (Ψ_s) of sap was calculated as $-nRT/V$, where n represents numbers of solute molecules; R represents the universal gas constant; T represents temperature in K, and V is volume in liter.

Leaf samples (200 mg FW) were ground in liquid nitrogen and homogenized in 1 ml of N,N-dimethylformamide. After 30 min of incubation under dark conditions, the homogenate was centrifuged at 10,000 rpm for 15 min at 4 °C. The absorbance of the supernatant was recorded at 461, 647, 664, and 664.5 nm. The contents of photosynthetic pigments were calculated following Inskeep and Bloom (1985) and Chamovitz et al. (1993).

Photosynthetic Gas Exchange Measurement

The photosynthetic gas exchange was recorded using a conifer chamber (6400-05 LCF, Li-Cor) attached to an infrared gas analyzer (LI-6400XT; Li-Cor, Lincoln, NE, USA). The plants under natural habitat exhibited the highest rate of photosynthesis at 1000 µmol m^{-2} s^{-1} PPFD (data not given); therefore, gas exchange was recorded at this intensity. Data were recorded on plants (10 replicates per stress treatment and 10 readings per replicate, $n = 100$) acclimatized to conifer chamber conditions for 20–30 min. Reads were recorded at 1000 µmol m^{-2} s^{-1} PPFD, 380 or 1200 µmol mol^{-1} CO_2, 26 ± 0.5 °C block temperature, and 60 ± 5% RH. The net photosynthesis rate (P_N; µmol CO_2 m^{-2} s^{-1}), stomatal conductance (g_s; mol H_2O m^{-2} s^{-1}), intercellular CO_2 concentration (C_i; µmol CO_2 mol air^{-1}), transpiration rate (E; mmol H_2O m^{-2} s^{-1}), ratio of C_i to available CO_2 concentration (C_i/CA), and vapor pressure deficit (VpdL) were determined. The water-use efficiency (WUE; µmol CO_2 $mmol^{-1}$ H_2O) was calculated as the ratio of P_N and E.

Chlorophyll a Fluorescence Measurement

Chlorophyll a fluorescence was recorded using Handy Plant Efficiency Analyser (HPEA; Hansatech Instruments, UK). Measurements were recorded at RT on adaxial surface of the intact leaves through continuous excitation with high time resolution to investigate the rapid fluorescence induction (Oukarroum et al. 2015). Before measurement, the plants were dark adapted for 45 min using dark-adaptation facilities. Leaves were illuminated with saturating red light of 3000 µmol (photon) m^{-2} s^{-1} to close PSII reaction centers (RC) completely, and fluorescence signals were recorded for 1.0 s on a 4 mm diameter area of the dark-adapted leaves. The fluorescence detector used 730 ± 15 wavelength of 3000 µmol (photon) m^{-2} s^{-1} intensity. The instrument recorded prompt fluorescence (PF) when actinic light was on (light interval) and off (dark interval), respectively. The data were downloaded into PEA Plus software (version 1.10) and analyzed using its data analysis module. Based on chlorophyll a fluorescence transient various photosynthetic fluxes

viz. plastoquinone pool size (area), minimal fluorescence (F_0), maximum fluorescence (F_M), variable fluorescence (F_V), basal quantum yield of non-photochemical processes in photosystem II (F_0/F_M), maximum quantum efficiency of PSII (F_V/F_M), activity of the water-splitting complex (F_V/F_0), absorption per RC (ABS/RC), electron transport flux per PSII RC (ET_0/RC), energy trapped in PSII RC (TR_0/RC), energy dissipated from PSII (DI_0/RC), and photochemical and non-photochemical de-excitation rate constant (k_P and k_N) were studied. The OJIP curve was plotted, and relative rise was interpreted as effects of the stress conditions on transfer of electron through PSII and PSI in plants under stress at aCO_2 and eCO_2. Amplitudes of *I–P* phase representing the ratio of PSII and PSI [$\delta F_{IP} = (F_P - F_I)$] and electron transport (δV_{IP}) around PSI to reduce final (i.e., ferredoxin and NADP) acceptors [$\delta V_{IP} = (F_m - F_{30ms})/(F_m - F_0)$] were determined following Schansker et al. (2005) and Khatri and Rathore (2019).

Determination of Proline, Sugar, Starch, and Polyphenol Contents

Proline contents from fresh leaf samples were extracted in 3.0% sulphosalicylic acid. The extract was reacted with ninhydrin reagent, and absorbance was read at 520 nm following Bates et al. (1973). Soluble sugar from samples was extracted repeatedly in 80% ethanol and estimated following anthrone-sulphuric acid method. The residual pellet left after extract of the soluble sugar was digested in 52% perchloric acid for starch estimation. The digest was diluted with milliQ water and processed as that of sugar estimation. Glucose was used as standard, and absorbance was read at 630 nm. For starch determination, the obtained values were multiplied by a factor of 0.9 to convert the glucose values into starch. Polyphenol contents were estimated following Chandler and Dodds (1983) by recording the absorbance at 650 nm against a standard curve prepared with catechol.

Determining the Expression of C_4 Photosynthetic Pathway Genes

Total RNA was extracted from leaf samples following the GITC method (Chomczynski and Sacchi 1987). The cDNA was prepared using total RNA as template and a Superscript II RT first-strand cDNA synthesis kit (Promega, Madison, Wisconsin). Expression of the *NADP-me* (F5′-TGCCCATAC CCCTTGAT-3′ and R5′-TTGGCAAAATCTTCGAACT-3′) and *NADP-mdh* (F5′-GCTTGCTTCTGGTGTGGT-3′ and R5′-CAATCAGAATGGCCCACT-3′) genes was determined using real-time PCR (RT-PCR). The tubulin (F5′-CACGCG CTGTATTCGTAGAT-3′ and R5`-TGACCACGAGCGAAG TTATTAG-3′) gene was used as an internal control. RT-PCR was performed using 1 × Sso Advanced SYBR green supermix (Bio-Rad). qRT-PCR conditions comprised denaturation at 94 °C for 5 min for 1 cycle; 40 cycles of each denaturation at 94 °C for 30 s (sec); annealing at 55 °C for 30 s; and extention at 72 °C for 30 s. Relative-fold expression was calculated using following Livak and Schmittgen (2001).

Statistical Analysis

The experiment was performed in a randomized block design with minimum 03 replicates (each replicate with 3 sub-replicates; $n = 9$) for physio-chemical estimations and with 10 replicates (each replicate with 10 sub-replicates; $n = 100$) for measurment of gas exchange and chlorophyll fluorescence. Data recorded were subjected to ANOVA for analysis of variance to determine the significance among mean values of the treated and control plants (Supplementary Table S1). Post-hoc multiple comparison of mean values was carried out following Tukey's test at a significance level of $p \leq 0.05$. To construct the radar plot (Fig. 9), the chlorophyll a fluorescence reads of control plants (under both levels of CO_2) were considered as standard and the reads of stress-treated plants were calculated as relative values. The data are presented as mean ± standard error (SE) and significantly different mean values have been denoted by different lowercase letters.

Results

The eCO_2 had differential effects on photosynthetic C capture potential, ion accumulation, physio-biochemical and growth responses in *S. fruticosa* and *S. monoica* under salt (100 mM NaCl and 50% strength of SW) and osmotic (10% PEG) stress. Leaf anatomy in both species showed differentiation of ground tissues as palisade and spongy mesophylls (Fig. 1a, b); however, none of these possess bundle sheath or *Kranz* anatomy (Fig. 1c, d).

Effect of eCO_2 on Growth and Water Content in *S. fruticosa* and *S. monoica*

S. fruticosa exhibited improved growth under saline conditions and *S. monoica* exhibited improved growth under seawater salinity (Fig. S2) at aCO_2. Similarly, both species showed improved growth at eCO_2; however, the growth in *S. monoica* was comparatively better as compared to *S. fruticosa* as the eCO_2 induced the epinastic symptoms in *S. fruticosa* leaves (Fig. S3). Similar to shoot growth, both species showed improved root growth under salinity stress at both levels of CO_2. At eCO_2, the SW salinity significantly improved the root growth in both species

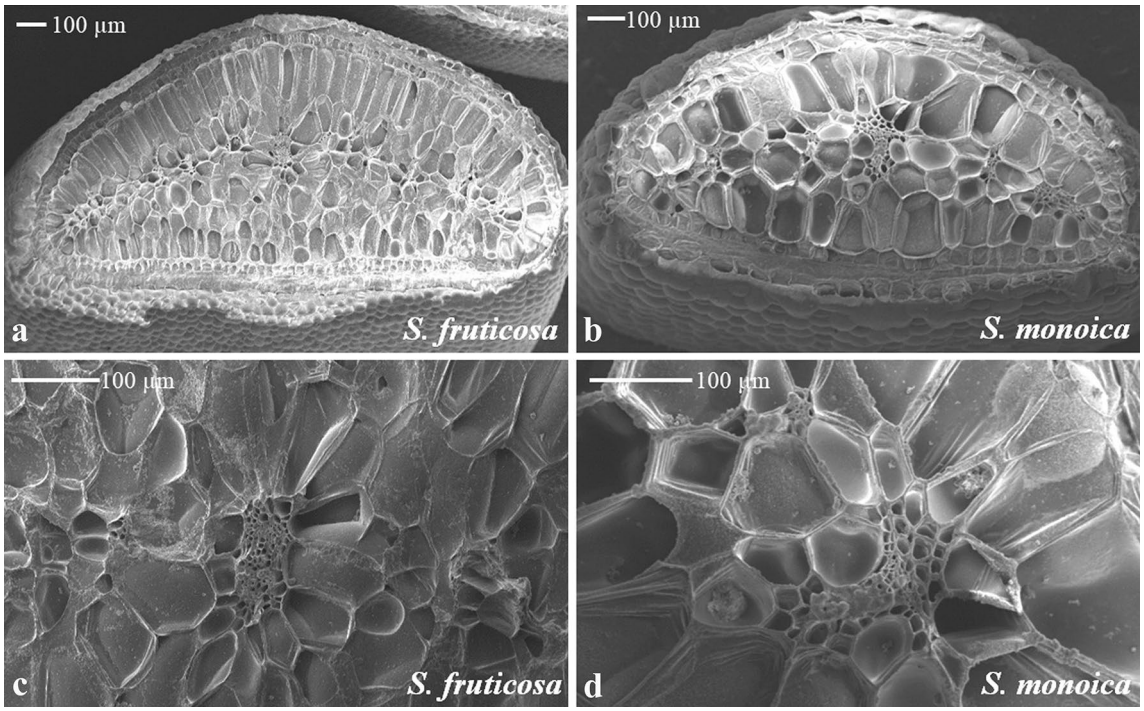

Fig. 1 The SEM-cryo images showing leaf anatomy (**a**, **b**) and the enlarged view of vascular tissues (**c**, **d**) in *S. fruticosa* and *S. monoica* respectively

(Fig. S4). *S. fruticosa* and *S. monoica* yielded FW and DW in agreement with growth (Fig. S5a, b). At aCO_2, the biomass accumulation in *S. fruticosa* was comparatively higher than *S. monoica* under saline conditions. The eCO_2 improved the biomass yield in both species under SW salinity. Compared with aCO_2 condition, both species exhibited lower WC under eCO_2. Compared with control treatment, *S. fruticosa* maintained higher WC under stress conditions at eCO_2, and *S. monoica* did not exhibit significant changes in WC (Fig. S5c). Both species exhibited poor growth attributes and WC under PEG stress. The interaction among *Suaeda* species, CO_2 levels, and stress type significantly influenced the plant growth, fresh and dry biomass yield, WC, and root growth.

Effect of eCO_2 on Carbon and Nitrogen Assimilation in *Suaeda* Species

Both species exhibited no significant variations in C contents under control and stress conditions at aCO_2. The eCO_2 reduced the C contents in *S. fruticosa* under stress conditions; however, *S. monoica* exhibited no significant variations (Fig. 2a). *S. fruticosa* showed comparatively lower accumulation of N contents, and *S. monoica* exhibited higher accumulation of N contents under saline conditions at eCO_2 (Fig. 2b). The interaction among *Suaeda* species, CO_2 levels, and stress treatments had significant influence over the accumulation of C and N contents. *S. fruticosa* and *S. monoica* exhibited the stable isotope ratio ($\delta^{13}C$) as − 21.44 and − 15.62, respectively.

Effect of eCO_2 on Ion Accumulation and Solute Potential in *Suaeda* Species

Both species accumulated higher contents of Na^+ and lower contents of K^+ under stress conditions (Fig. 3b, c). The eCO_2 significantly reduced accumulation of Na^+ and K^+ in both species under stress. The EDX-SEM observations confirmed the higher accumulation of Na^+ and lower accumulation of K^+ in leaf tissues and on root surface of both species under saline condition (Fig. S6). In agreement with ion accumulation, *S. fruticosa* and *S. monoica* exhibited significantly lower Ψ_s (more negative values) under stress condition at both levels of CO_2 (Fig. 3a). The decrease in Ψ_s under stress condition was comparatively higher in both species at aCO_2 than eCO_2. The interactions among *Suaeda* species, CO_2 levels, and stress type significantly influenced the Ψ_s and accumulation of ions.

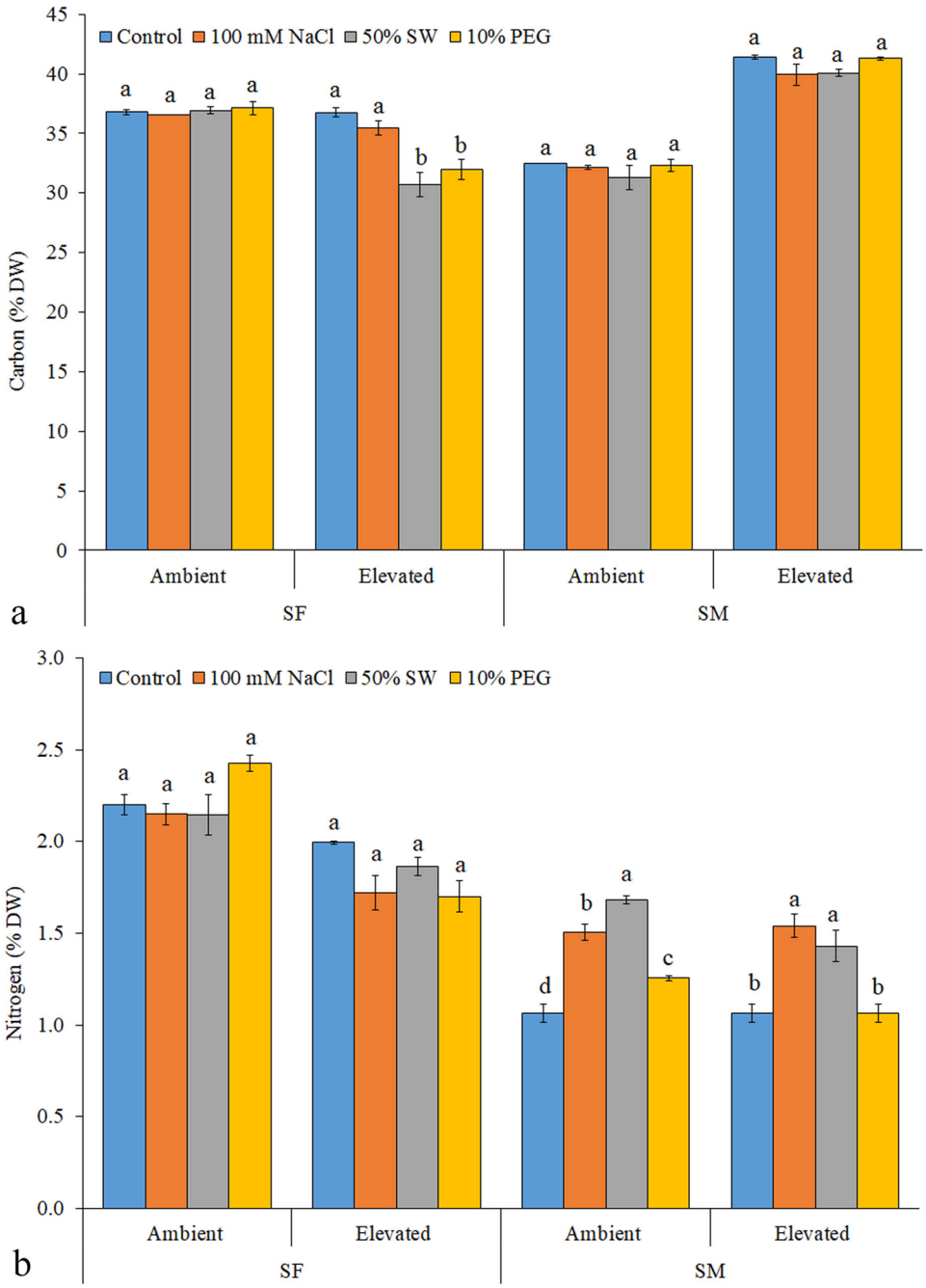

Fig. 2 Carbon (**a**), and nitrogen (**b**) contents in *S. fruticosa and S. monoica* under control and stress (100 mM NaCl, 50% seawater salinity and 10% PEG) treatments at ambient and elevated CO_2 condition for 7 days. The values (mean ± SE, $n = 3$) followed by different lowercase letters as superscripts are significantly different by LSD ($\geq 0.05\%$) at a particular CO_2 level. In figure, SW represents seawater salinity, *SF S. fruticosa*, and *SM S. monoica*

Effect of eCO_2 on ROS Accumulation and Membrane Properties in *Suaeda* Species

Stress induces accumulation of O_2^- and H_2O_2 in *S. fruticosa* and *S. monoica* at both levels of CO_2. NaCl stress caused comparatively higher accumulation of O_2^- (Fig. 4a). *S. fruticosa* exhibited higher accumulation of H_2O_2 under stress at eCO_2 while *S. monoica* exhibited higher accumulation at aCO_2 (Fig. 4b). *S. monoica* exhibited higher accumulation of O_2^- and H_2O_2 under NaCl stress at both levels of CO_2. At eCO_2, *S. monoica* exhibited similar accumulation of ROS under control and saline condition. At eCO_2, *S. monoica* under PEG stress exhibited higher accumulation of superoxide and lower accumulation of peroxide radicals.

S. monoica exhibited lower MDA contents under stress condition at aCO_2. Stress increased the accumulation of MDA in *S. fruticosa* at both levels of CO_2 except PEG stress at eCO_2. *S. monoica* exhibited lower contents of MDA under stress condition at aCO_2. In contrary to aCO_2, the eCO_2 significantly increased the MDA accumulation in *S. monoica* under 50% SW. The eCO_2 increased MDA content in *S. fruticosa* and *S. monoica* under NaCl and SW

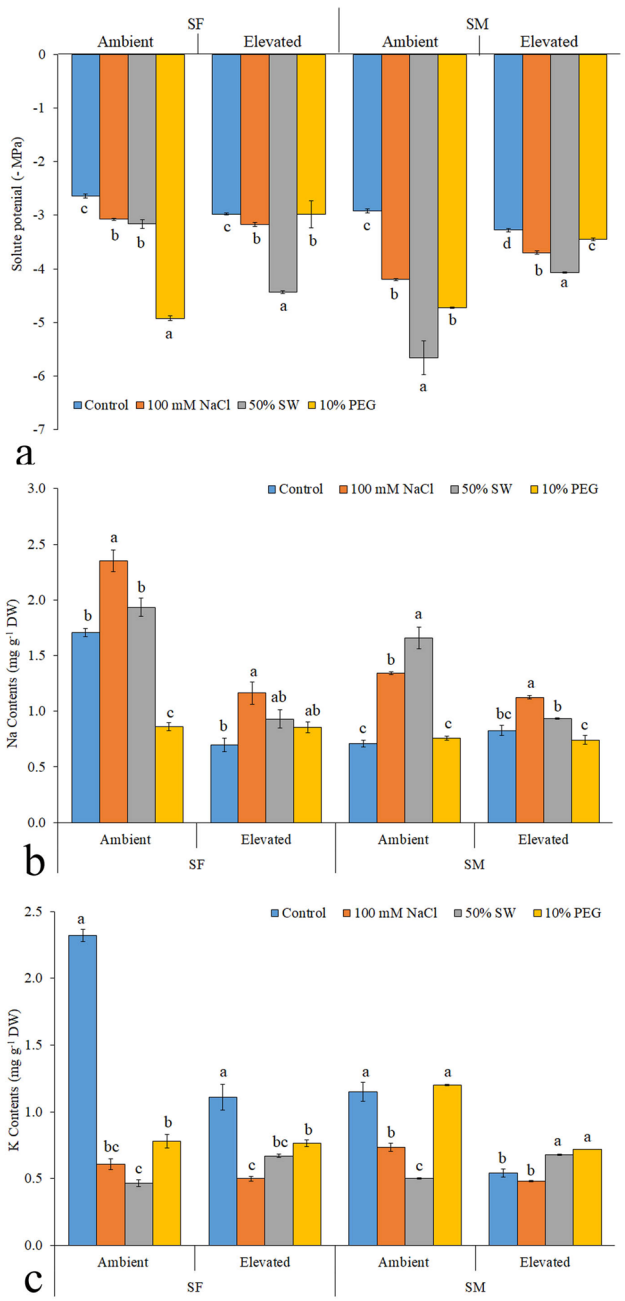

Fig. 3 Solute potential (**a**) and accumulation of sodium (**b**) and potassium (**c**) contents in leaves of *S. fruticosa and S. monoica* under control and stress (100 mM NaCl, 50% seawater salinity, and 10% PEG) treatments at ambient and elevated CO_2 condition for 7 days. The values (mean ± SE, $n = 3$) followed by different lowercase letters as superscripts are significantly different by LSD (≥ 0.05%) at a particular CO_2 level. In figure, SW represents seawater salinity, *SF S. fruticosa*, and *SM S. monoica*

stress, respectively (Fig. 5a). The eCO_2 increased the EL in *S. fruticosa* under stress; however, *S. monoica* exhibited lower EL at both levels of CO_2 under stress. NaCl stress caused higher EL than SW stress in both species at aCO_2 (Fig. 5b). The eCO_2 significantly reduced the EL in *S. monoica* under salinity stress compared with osmotic stress. The interaction among *Suaeda* species, CO_2 levels, and stress type had a significant effect on MDA accumulation and EL.

Effect of eCO_2 on Expression of C_4 Pathway Genes and Activity of Antioxidant Enzymes

S. fruticosa and *S. monoica* exhibited up-regulation of *NADP-me* and *NADP-mdh* gene at both levels of CO_2 under stress (Fig. 6). Both species showed the highest (more than sixfold changes) expression of *NADP-me* and *NADP-mdh* under SW salinity at eCO_2. Stress induced the up-regulation of *NADP-me* and *NADP-mdh* gene in both species at both levels of CO_2. Compared with aCO_2, the eCO_2-induced up-regulation of both genes in *S. monoica* under PEG stress.

At aCO_2, both species exhibited higher activity of SOD and CAT under stress; however, GPOX exhibited higher activity only under NaCl stress. Plants of both species under control treatment exhibited higher activity of SOD, CAT, and GPOX at eCO_2 as compared to aCO_2 (Fig. 7). Similarly, both species have higher antioxidant enzymes activity under stress condition at eCO_2; however, *S. fruticosa* showed lower activity of CAT under stress condition. Difference in the activity of these enzymes varied with types of stress and plant species.

Effect of eCO_2 on Photosynthetic Pigments in *Suaeda* Species

S. fruticosa exhibited lower accumulation of chlorophyll and carotenoid pigments under stress condition except for NaCl stress at aCO_2. The eCO_2 improved the accumulation of photosynthetic pigments in *S. fruticosa* under stress condition (Fig. S7a, b); however, under NaCl stress, increase in the pigments was not statistically significant. The aCO_2 and eCO_2 have no significant effect on accumulation of total chlorophyll in *S. monoica* under stress condition. *S. fruticosa* showed higher accumulation of carotenoids under NaCl at aCO_2 and under stress condition at eCO_2 (Fig. S7b). *S. monoica* accumulated significantly higher content of carotenoids under PEG stress at aCO_2 and under stress condition at eCO_2 (Fig. S7b). *Suaeda* species, CO_2 levels and stress type showed significant interaction for the accumulation of total chlorophyll and carotenoid contents.

Effect of eCO_2 on Photosynthesis in *Suaeda* Species

The CO_2 levels and stress types had differential effects on photosynthetic gas exchange in *S. fruticosa* and *S. monoica*. SW salinity improved the P_N in *S. fruticosa* at both level of CO_2; however, the increase was not significant. PEG and NaCl stress decreased the P_N in *S. fruticosa*

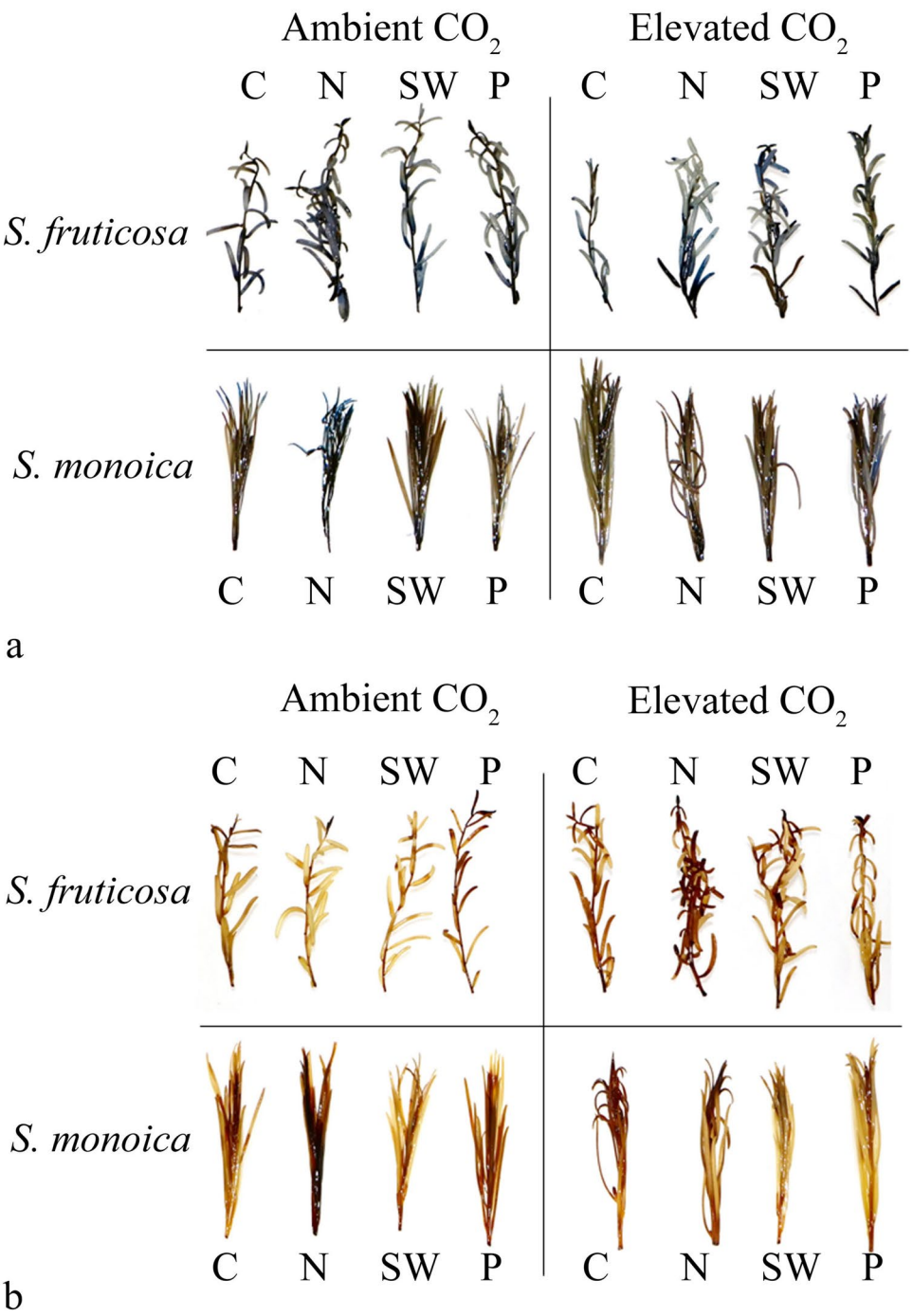

Fig. 4 In vivo detection of superoxide radials by NBT assay (**a**) and peroxide by DAB assay (**b**) in shoot apical portions of *S. fruticosa and S. monoica* grown under control and stress (100 mM NaCl, 50% seawater salinity, and 10% PEG) treatments at ambient and elevated CO_2 conditions for 7 days. In figure, the C represents control, *N* NaCl, *SW* seawater salinity, and *P* PEG

at both level of CO_2. Salinity stress improved the P_N in *S. monoica* at both levels of CO_2; however, the improvement was only significant under SW salinity at eCO_2. Compared with control plants, both species exhibited lower P_N under PEG stress at both levels of CO_2 (Fig. 8a); however, the reduction in P_N was significant only at aCO_2. *S. fruticosa* showed significantly higher g_s under SW salinity and lower g_s under PEG stress at aCO_2. There were no significant changes in g_s under stress at eCO_2. *S. monoica* showed higher g_s under stress conditions at aCO_2 and lower g_s under stress conditions at eCO_2 except NaCl stress (Fig. 8b). *S. fruticosa* showed lower C_i under stress conditions at aCO_2, while *S. monoica* showed lower C_i under stress conditions at eCO_2 except NaCl stress. Compared with plants under control treatment, the *S. fruticosa* had higher C_i under stress condition at eCO_2 and *S. monoica* had higher C_i under stress condition at aCO_2 (Fig. 8c). *S. fruticosa* and *S. monoica* exhibited *E* in a trend as that of g_s (Fig. 8d). *S. fruticosa* exhibited lower WUE under stress at both levels of CO_2. *S. monoica* had

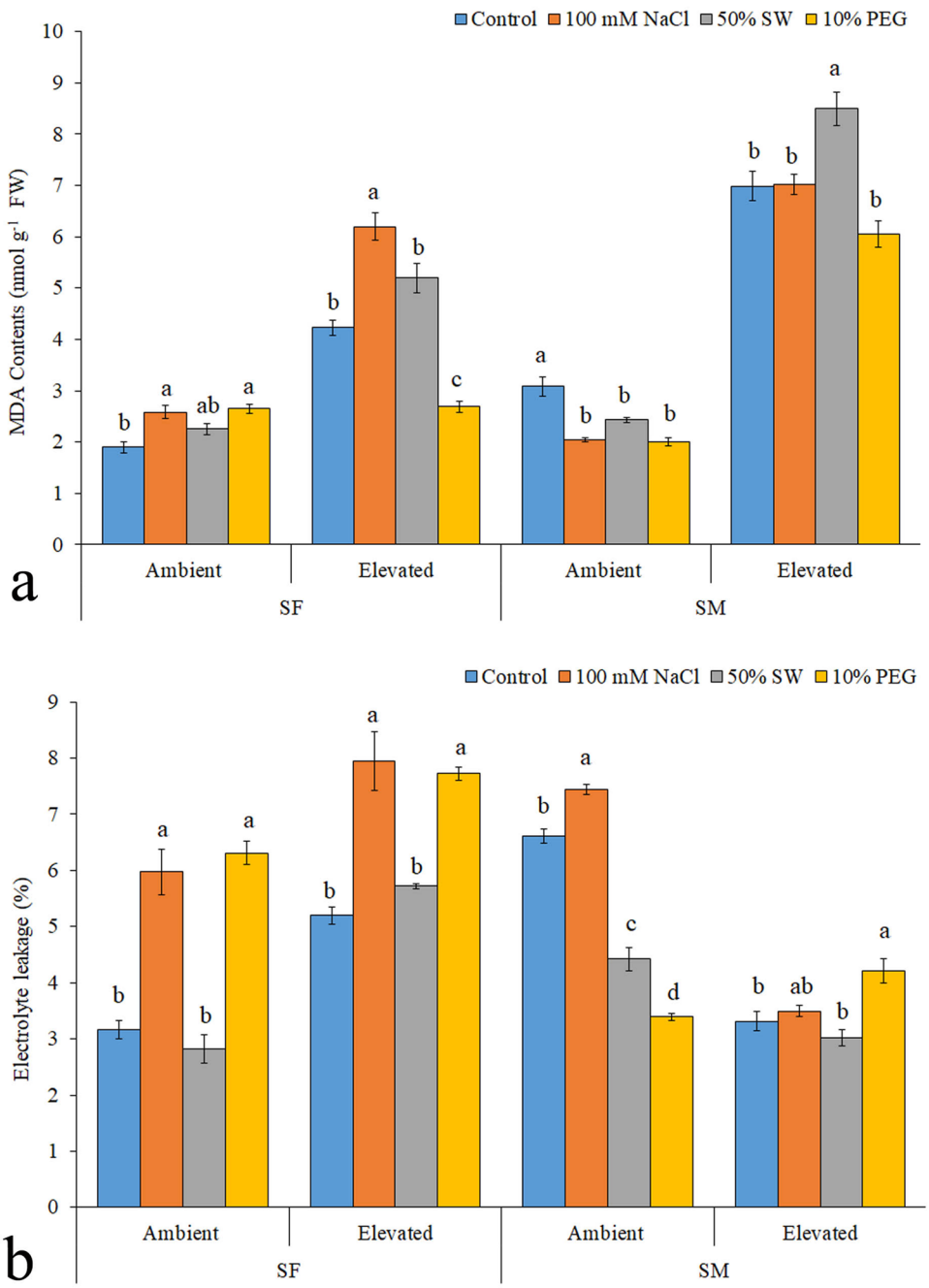

Fig. 5 MDA contents (**a**) and electrolyte leakage (**b**) in leaves of *S. fruticosa and S. monoica* under control and stress (100 mM NaCl, 50% seawater salinity, and 10% PEG) treatments grown at ambient and elevated CO_2 condition for 7 days. The values (mean ± SE, $n = 3$) followed by different lowercase letters as superscripts are significantly different by LSD (≥ 0.05%) at a particular CO_2 level. In figure, SW represents seawater salinity, *SF S. fruticosa*, and *SM S. monoica*

lower WUE under stress at aCO_2. *S. monoica* under stress showed WUE comparable to control or higher than control at eCO_2. Both species exhibited C_i/CA in a trend as that of C_i. Both species showed VpdL almost comparable in plants under control and stress conditions at both levels of CO_2 (Fig. S8a–c). Stress treatments and their interaction with CO_2 levels had a significant effect on P_N and WUE. Similarly, interaction among *Suaeda* species, CO_2 levels, and stress treatments had a significant effect on g_s, C_i, E, C_i/CA, and VpdL.

Effect of eCO_2 on Chlorophyll a Fluorescence in *Suaeda* Species

S. fruticosa and *S. monoica* showed variable chlorophyll a fluorescence transient, chlorophyll fluorescence parameter, and different photosynthetic flux under salinity and PEG stress at aCO_2 and eCO_2 (Fig. 9a–d). Under stress, *S. fruticosa* showed higher pool size of electron acceptors (Q_A) on reducing side of PSII (area) at aCO_2 and lower at eCO_2. In contrary, *S. monoica* showed reduced area at aCO_2 and improved area at eCO_2 under stress. Both species showed

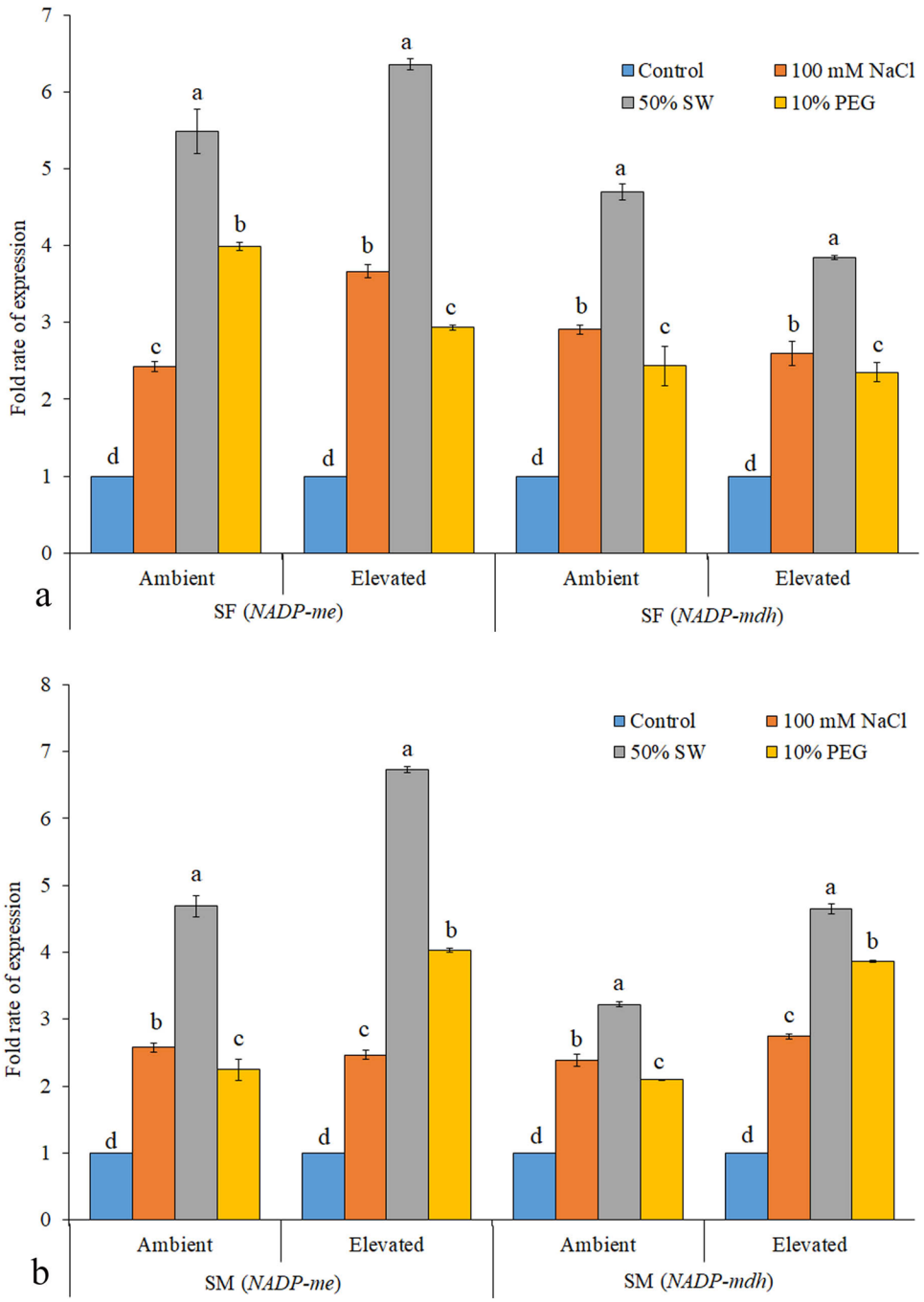

Fig. 6 Gene expression profiling of NADP-dependent malic enzyme (*me*) and malate dehydrogenase (*mdh*) in *S. fruticosa* (**a**) and *S. monoica* (**b**) under control and stress (100 mM NaCl, 50% seawater salinity, and 10% PEG) treatments at ambient and elevated CO_2 condition for 7 days. The values (mean ± SE, $n = 3$) followed by different lowercase letters as superscripts are significantly different by LSD ($\geq 0.05\%$) at a particular CO_2 level. In figure, SW represent seawater salinity, *SF S. fruticosa*, *SM S. monoica*, *ME* malic enzyme, and *MDH* malate dehydrogenase

higher F_0 under stress at both levels of CO_2 except NaCl stress in *S. fruticosa* and SW salinity in *S. monoica* at aCO_2. *S. monoica* exhibited lower F_M and F_V under stress at aCO_2. *S. fruticosa* at both levels of CO_2 and *S. monoica* at eCO_2 exhibited higher F_M and F_V under stress. *S. fruticosa* exhibited lower F_0/F_M under stress at both levels of CO_2. *S. monoica* had lower estimates of F_0/F_M under NaCl and PEG stress at eCO_2. *S. fruticosa* at aCO_2 and *S. monoica* at eCO_2 yielded higher estimates of F_V/F_M and F_V/F_0 under stress. In contrary, *S. monoica* at aCO_2 and *S. fruticosa* at eCO_2 yielded lower estimates of F_V/F_M and F_V/F_0 under stress. *S. fruticosa* under stress showed higher F_V/F_0 at aCO_2 and lower at eCO_2. *S. monoica* yielded lower estimates of F_V/F_M under stress at aCO_2 and under SW salinity at eCO_2. Both plant species showed higher ABS/RC, DI_0/RC, and TR_0/RC under stress at both levels of CO_2. *S. fruticosa* had higher ET_0/RC under stress at both levels of CO_2, while *S. monoica* at aCO_2. Contrary to *S. fruticosa*, the *S. monoica* showed lower ET_0/RC under stress at eCO_2 level.

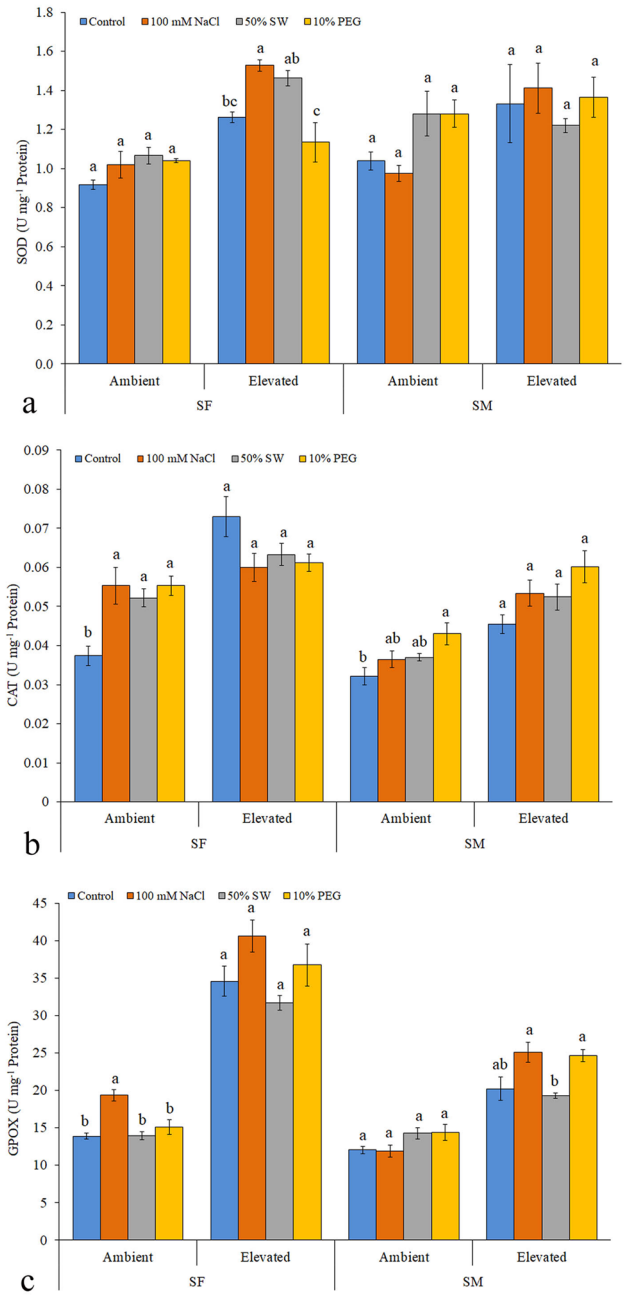

Fig. 7 Activity of superoxide dismutase (**a**), catalase (**b**), and guaiacol peroxidase (**c**) in *S. fruticosa and S. monoica* under control and stress (100 mM NaCl, 50% seawater salinity and 10% PEG) treatments at ambient and elevated CO_2 for 7 days. The values (mean ± SE, $n = 3$) followed by different lowercase letters as superscripts are significantly different by LSD (≥ 0.05%) at a particular CO_2 level. In figure, SW represents seawater salinity, *SF S. fruticosa*, and *SM S. monoica*

S. fruticosa showed higher K_P/ABS, and *S. monoica* showed lower K_P/ABS under stress at eCO_2.

OJIP transient curves based on PF data of *S. fruticosa* and *S. monoica* under stress at aCO_2 and eCO_2 are presented in Fig. S9. *S. fruticosa* showed lower relative rise in O to J phase under stress at aCO_2 and exhibited the lowest rise in plants under PEG stress. *S. monoica* showed the highest relative rise in O to J phase under SW salinity stress at aCO_2 and followed by unstressed plants. *S. fruticosa* showed the lowest relative rise in O to J phase under PEG stress at eCO_2. *S. monoica* showed the highest relative rise in O to J phase under PEG stress at eCO_2 and plants under SW and NaCl treatments followed this. *S. fruticosa* had higher δF_{IP} under stress at aCO_2. At eCO_2, it showed significantly lower δF_{IP} under stress except SW salinity as compared to control plants (Fig. S10a). *S. monoica* did not exhibit a significant change in δF_{IP} under stress at aCO_2, while at eCO_2, it showed a significant increase in δF_{IP} under saline condition. *S. fruticosa* showed a significantly lower δV_{IP} under PEG stress at aCO_2. *S. monoica* did not exhibit changes in δV_{IP} under stress at aCO_2. Both species exhibited significantly higher δV_{IP} under SW salinity and PEG stress at eCO_2 (Fig. S10b).

Effect of eCO_2 on Accumulation of Sugar, Starch, Proline, and Polyphenol

Saline conditions induced accumulation of sugar in *S. fruticosa* at aCO_2. The eCO_2 lowered the accumulation of soluble sugar in *S. fruticosa* under stress except NaCl treatment. *S. fruticosa* showed higher accumulation of total sugar under saline conditions at aCO_2; however, *S. monoica* exhibited lower accumulation under stress. *S. monoica* showed lower accumulation of soluble sugar under stress at eCO_2 except SW salinity (Fig. 10a); however, reduction was not statistically significant. *S. fruticosa* accumulated higher contents of starch under stress at aCO_2, while accumulation decreased at eCO_2. *S. monoica* exhibited lower accumulation of starch under SW and PEG stress at aCO_2, while it exhibited significantly higher accumulation under SW salinity at eCO_2 (Fig. 10b). *S. fruticosa* exhibited higher accumulation of proline and polyphenol contents under stress at both levels of CO_2 (Fig. 10c, d). The eCO_2 increased the proline accumulation in *S. monoica* under saline condition at aCO_2, and all the imposed strengths of stresses at eCO_2. The polyphenol accumulation increased in *S. monoica* under saline condition at aCO_2 and under SW and PEG stress at eCO_2. The interaction among *Suaeda* species, CO_2 levels, and stress type had a significant effect on the accumulation of total soluble sugar, starch, proline, and polyphenol contents.

Discussion

The eCO_2 induced differential growth, physio-chemical, and photosynthetic responses in *S. fruticosa* and *S. monoica* under 100 mM NaCl/50% strength of SW/10% PEG-induced stress (Supplementary Table S2). The leaf anatomy clearly

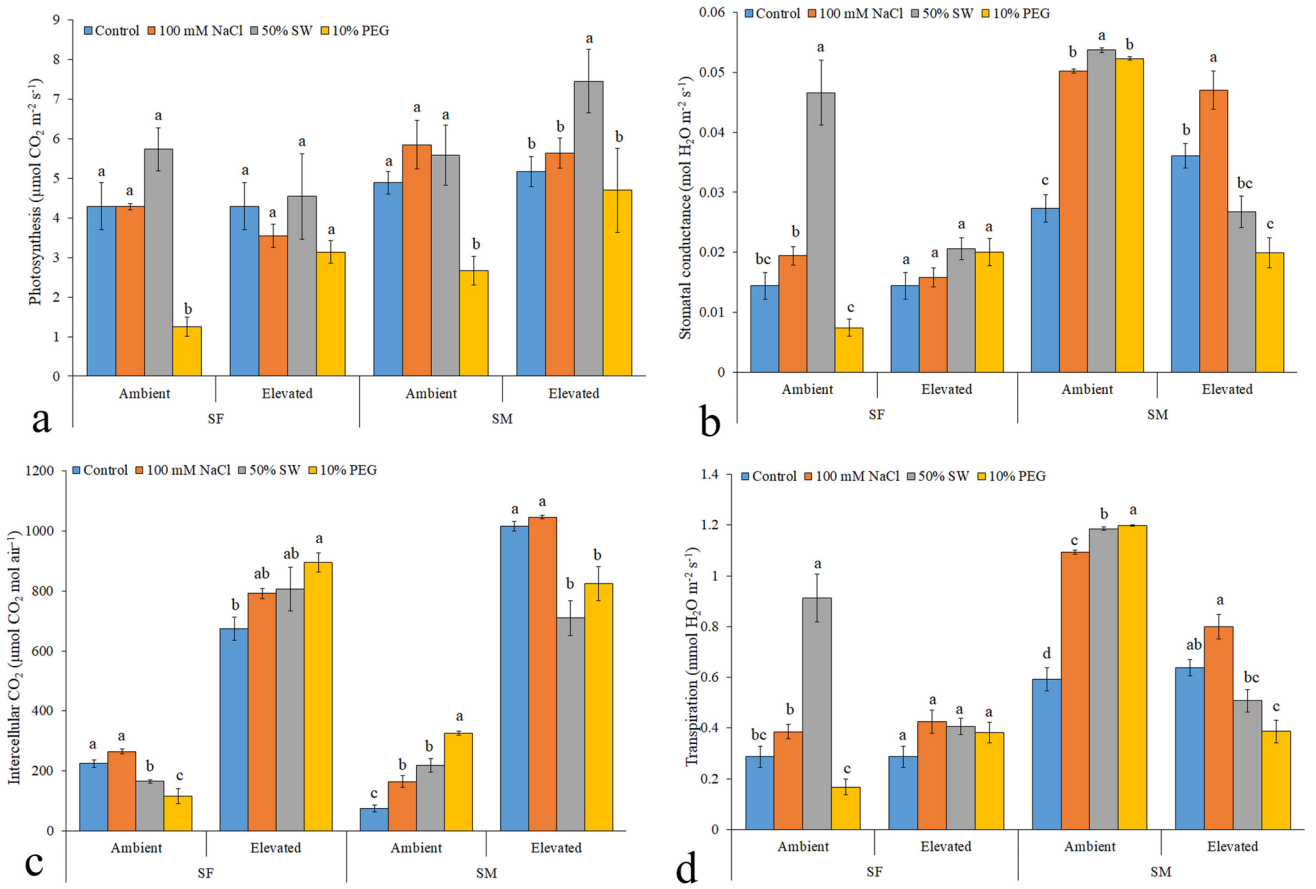

Fig. 8 Net photosynthesis rate (**a**), stomatal conductance (**b**), intercellular co_2 concentration (**c**) and transpiration (**d**) in leaves of *S. fruticosa and S. monoica* under control and stress (100 mM NaCl, 50% seawater salinity and 10% PEG) treatments at ambient and elevated CO_2 for 7 days. The values represent mean ± SE ($n = 3$) and followed by different letters as superscripts are significantly different by LSD (≥ 0.05%) at a particular CO_2 level. In figure, SW is seawater salinity, *SF S. fruticosa*, and *SM S. monoica*

demonstrated the absence of typical *Kranz* anatomy in both species indicating it as a non-essential criterion in determining the type of C fixation in *Suaeda* species. The $\delta^{13}C$ estimates supported the operation of C_4 mode of CO_2 fixation in *S. monoica* (Shomer-Ilan et al. 1975; Voznesenskaya et al. 2002) and C_3 or intermediate pathway of CO_2 fixation in *S. fruticosa* (Stutz et al. 2014). The $\delta^{13}C$ estimates indicated the efficiency of CO_2 fixation in *Suaeda*. The better growth, eco-physiological responses, and absence of the epinastic symptoms indicated higher photosynthetic efficiency in *S. monoica* at eCO_2 and better utilization of CO_2.

Stress induces accumulation of inorganic solutes and synthesis of different compatible solutes. The ionomic analysis clearly showed a higher accumulation of Na^+ and lower accumulation of K^+ under saline stress (Haque et al. 2017; Rathore et al. 2019). The accumulated inorganic solutes contribute to the osmotic adjustment after compartmentalization to avoid the cellular toxicity (Haque et al. 2017; Keisham et al. 2018). Lower solute potential helped plants to conserve and efficiently utilize the available water under physiological drought (Kumari et al. 2017; Rathore et al. 2019). The saline condition induced growth, and this indicated requirement of salts for optimum growth in *Suaeda* species (Haque et al. 2017; Rathore et al. 2019; Jacob et al. 2020). In consonance with present results, 100–300 mM NaCl salinity did not cause injuries in *S. glauca* and plants grew better (Jin et al. 2016). Similarly, the eCO_2 improved the growth and biomass accumulation in both C_3 and C_4 species of *Atriplex, Phaseolus*, *Xanthium,* and *Zea mays* under saline condition (Schwarz and Gale 1983; Li et al. 2014). These results indicated the operation of an efficient mode of CO_2 fixation in *S. monoica* as compared to *S. fruticosa* (Schwarz and Gale 1983), and this resulted in superior performance of *S. monoica* under stress at eCO_2.

Stress caused oxidative damages through ROS accumulation adversely affects the physiology of plants and damages the photosynthetic machinery, thus, resulting in reduced growth (Ahammed et al. 2020c). The higher activity of antioxidant enzymes in both species under stress sequestered the ROS and combated the oxidative stress. Lower MDA

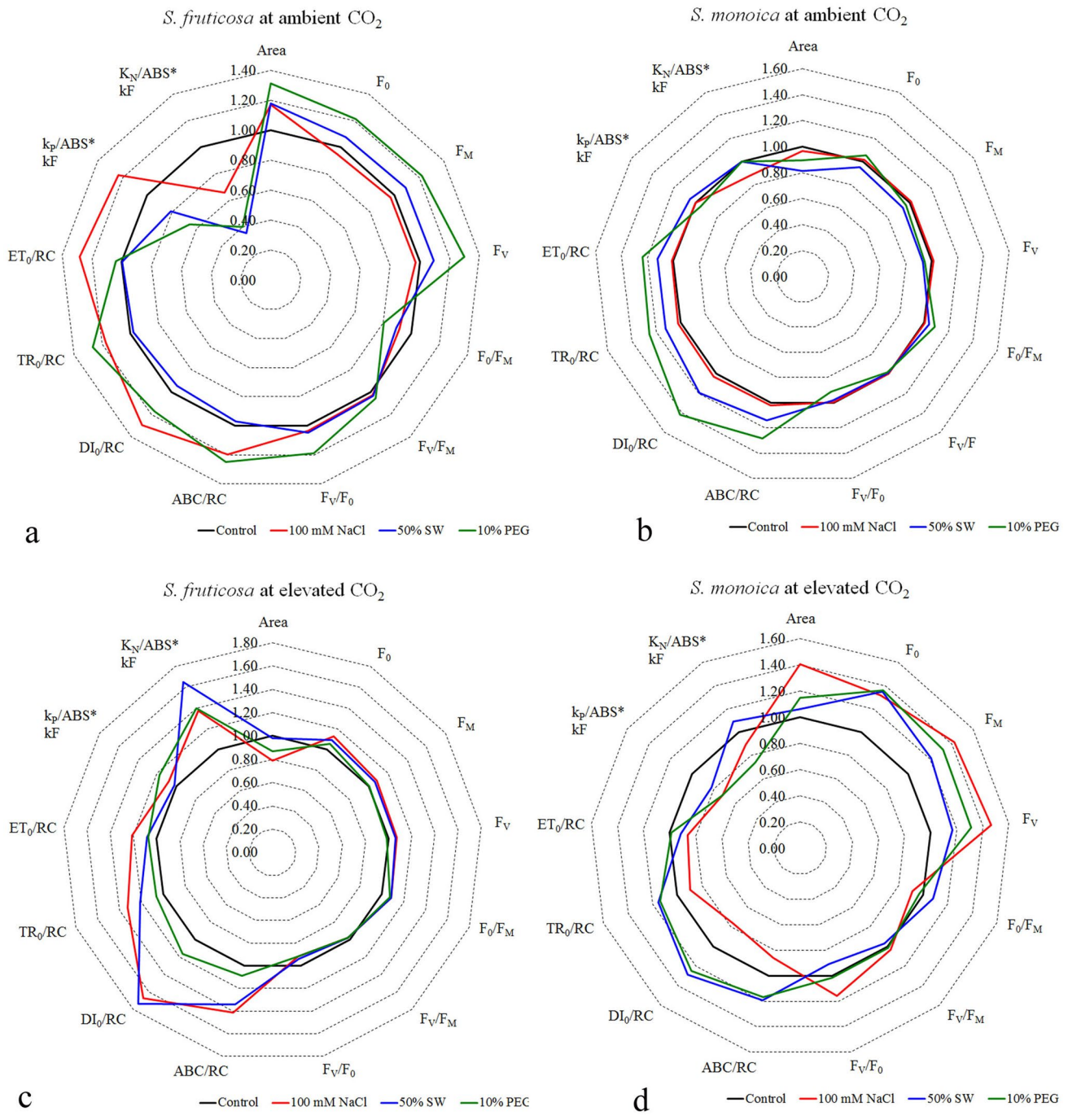

Fig. 9 Chlorophyll a fluorescence derived parameters and fluxes in *S. fruticosa* and *S. monoica* under control and stress (100 mM NaCl, 50% seawater salinity and 10% PEG) treatments at ambient (**a**, **b**) and elevated CO_2 (**c**, **d**) for 7 days. The values represent mean ± SE ($n = 10$) and followed by different letters as superscripts are significantly different by LSD (≥ 0.05%) at a particular CO_2 level. In figure, SW is seawater salinity. In picture, the area represents plastoquinone pool, F_0—minimal fluorescence, F_M—maximum capacity for photochemical quenching, F_V—variable fluorescence, F_0/F_M—basal quantum yield of non-photochemical processes in PSII, F_V/F_M—maximum quantum efficiency of PSII, F_V/F_0—activity of the water-splitting complex, ABS/RC—absorption per RC, ET_0/RC—electron transport flux per PSII RC, TR_0/RC—energy trapped in PSII RC, DI_0/RC—energy dissipated from PSII, and k_P and k_N—photochemical and non-photochemical de-excitation rate constant

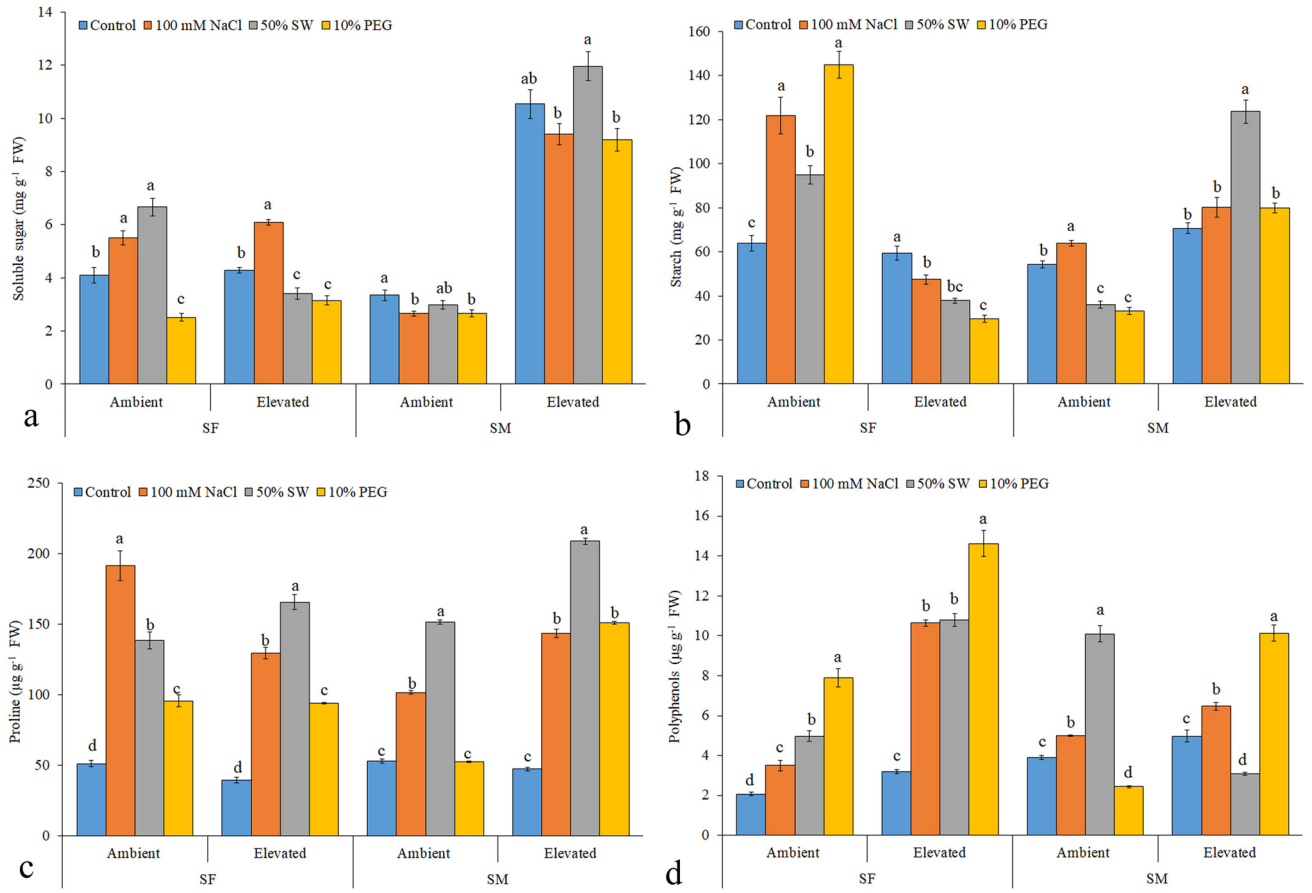

Fig. 10 Accumulation of soluble sugar (**a**), starch (**b**), proline (**c**), and polyphenol (**d**) contents in *S. fruticosa and S. monoica* under control and stress (100 mM NaCl, 50% seawater salinity and 10% PEG) treatments at ambient and elevated CO_2 condition for 7 days. The values (mean ± SE, $n = 3$) followed by different lowercase letters as superscripts are significantly different by LSD (≥ 0.05%) at a particular CO_2 level. In figure, SW represents seawater salinity, *SF S. fruticosa*, and *SM S. monoica*

accumulation and EL in *S. monoica* under stress condition at both levels of CO_2 clearly indicated a lower degree of ROS-induced membrane damages, which indicated improved efficiency of the photosynthetic machinery. In consonance with present results, the eCO_2 significantly curtailed the accumulation of ROS and MDA (Singh and Agrawal 2015). Lower accumulation of ROS might be a result of efficient utilization of light energy with available CO_2 which otherwise generates free radicals and damage the membrane integrity, photosynthetic machinery, and PSII system. The eCO_2-induced reduction in accumulation of ROS and MDA and the degree of EL are the indicators of efficient growth performances in *S. monoica* under stress. The present results clearly indicated role of eCO_2 in effective management of ROS, better acclimatization, and efficient photosynthetic responses in *S. monoica* as compared to *S. fruticosa* under stress.

Photosynthetic pigments are visual indicators of photosynthetic performance in plants. Higher contents of photosynthetic pigments contribute efficient harvesting of light energy required for fixation of the available CO_2 in photosynthesis (Ahammed et al. 2020c). The carotenoids sequester the free radicals (ROS) and acts as stress signaling molecule (the β-cyclocitral, an oxidation product of β-carotene) to induce the gene expression leading stress acclimation (Havaux et al. 2014). Compared with *S. fruticosa*, the *S. monoica* exhibited efficient photosynthetic CO_2 fixation (P_N) under stress indicating the operation of efficient CO_2 fixation. The higher P_N, lower C_i, and g_s in *S. monoica* under stress indicated better C utilization (Ueno et al. 2006). The efficient CO_2 fixation in *S. monoica* helped to maintain better P_N under lower estimates of g_s, C_i, and E at eCO_2 under stress. Vice versa, results in *S. fruticosa* indicated the operation of an intermediate CO_2 fixation pathway, which might not be as efficient as that of *S. monoica*. The eCO_2 increased the WUE in *S. monoica* under SW and PEG stress, which helped in water conservation and adaptation under physiological drought. In consonance with present results, the eCO_2 improved the photosynthesis in *Aster tripolium* and *Suaeda* species (Rozema et al. 1991; Yadav et al. 2018). Compared with *S. fruticosa*, the eCO_2 helped

in accumulation of higher contents of C in *S. monoica*; however, the N contents were lower. The accumulation of compatible solutes and their role in osmotic adjustment and sequestration of free radicals have been reported during stress tolerance in halophytes (Hong et al. 2000; Ashraf and Harris 2004; Moghaieb et al. 2004; Song et al. 2006; Ksouri et al. 2007; Lokhande et al. 2011; Haque et al. 2017; Rathore et al. 2019; Jacob et al. 2020). The higher content of starch in *S. monoica* at eCO_2 indicated the availability of sugar as raw material for starch synthesis, and this might be due to eCO_2-induced efficient photosynthesis. Up-regulations of *SmNADP-me* and *SmNADP-mdh* genes indicated operation of C_4 pathway and involvement of these genes in stress tolerance probably through enhancing the photosynthetic assimilates (Schwarz and Gale 1983; Wheeler et al. 2005; Rondeau et al. 2005). Expression of PEPC and PPDK enzymes have already been reported higher in *Suaeda* species under abiotic stress and eCO_2, respectively (Cheng et al. 2016; Yadav et al. 2018). Present results clearly indicated the role of eCO_2 in betterment of photosynthetic responses in *S. monoica* under stress. Compared with *S. fruticosa*, photosynthetic gas exchange measurements clearly indicated the better photosynthetic C-sequestration potential in *S. monoica* under stress at both levels of CO_2.

The CO_2 and stress induced variable changes in chlorophyll a fluorescence, photosynthetic fluxes, and OJIP transient in *S. fruticosa* and *S. monoica*. Under stress, eCO_2 improved the pool size in *S. monoica* indicating the efficient electron transfer at PSII donor side. The reduced pool size in *S. fruticosa* at eCO_2 indicated blockage of electron transfer from RC to quinone pool in *S. fruticosa* (Mehta et al. 2010; Khatri and Rathore 2019). Higher minimal fluorescence (F_0) indicated damage to the PSII (Bussotti et al. 2011) and heat dissipation in an uncontrolled manner resulting over excitation of RC in both species under stress. The higher F_0 and ABC/RC indicated improved antenna size with RCs, and this might be due to higher contents of photosynthetic pigments. The eCO_2-induced increase in photochemical quenching (F_M) indicated effective electron transport at PSII donor side and improved pool size of Q_A which supported the efficient utilization of accumulated $P680^+$ (Govindjee 1995) in both species and resulted in lower non-photochemical quenching. The lower estimate of F_0/F_M in *S. monoica* under stress indicated eCO_2-induced reduction in non-photochemical quenching (Ranjbarfordoei et al. 2006). These results indicated better abiotic stress tolerance in *S. monoica* at eCO_2. The higher F_V/F_M indicated efficient working of the photosynthetic machinery in *S. fruticosa* at aCO_2 and in *S. monoica* at eCO_2 under stress conditions (Salvatori et al. 2014; Khatri and Rathore 2019). F_V/F_M indicated better photosynthetic functioning of PSII RCs in *S. monoica* at eCO_2 under stress conditions. The water availability, pigment contents, and active and inactive RCs significantly influence the ABC/RC and F_0 under which indicated the improved antenna size (Misra et al. 2001). A higher number of inactive RCs contribute dissipation of heat energy, thus, higher DI_0/RC (Mathur et al. 2013). The eCO_2 helps *S. monoica* to maintain higher number of active RCs. The higher TR_0/RC indicated inefficiency of re-oxidation of reduced Q_A^- to Q_B resulting in loss of energy as dissipation (Mathur et al. 2013). Besides higher estimates of TR_0/RC and DI_0/RC, in the present case, the higher ABC/RC corresponded efficient photosynthesis, and this clearly indicated efficient light harvest by RCs and its downstream utilization for CO_2 fixation. Saline condition has been reported to have differential effects on electron transport (ET_0/RC) flux (Mathur et al. 2013; Demetriou et al. 2007; Khatri and Rathore 2019). Stress-imposed inactivation of RCs might be a reason for lower ET_0/RC in *S. monoica* under stress conditions at eCO_2 (Mehta et al. 2010). The rise in O to J phase in OJIP transient curves clearly showed a better reduction of Q_A by PSII in both species at aCO_2. The relative rise in O to J phase indicated better reduction of Q_A by PSII RCs in *S. monoica* at eCO_2 and under 10% PEG, seawater and NaCl treatments. The δF_{IP} in *S. fruticosa* at aCO_2 and in *S. monoica* at eCO_2 under stress conditions indicated better ratio of PSII and PSI (Schansker et al. 2005). The δV_{IP} in *S. monoica* under stress at eCO_2 indicated improved electron transport through PSI for reduction of final acceptors, i.e., ferredoxin and NADP (Schansker et al. 2005). Chlorophyll a fluorescence indicated comparatively reduced biophysical performances of photosynthetic system in *S. fruticosa* under stress, while *S. monoica* exhibited operation of an efficient photosynthetic system under stress conditions at both levels of CO_2.

The present results clearly indicated that the photosynthetic C fixation under stress directly influences the stress tolerance. The eCO_2 improved the growth and biomass accumulation in both species under stress; however, the performance of *S. monoica* was better as compared to *S. fruticosa* under eCO_2. The eCO_2-induced C and N assimilation in *S. monoica* under stress clearly indicated efficient functioning of photosynthetic machinery. The results demonstrated the efficient functioning of C concentration mode in *S. monoica*, which might be the major reason for eCO_2-induced better physio-chemical and photosynthetic responses in *S. monoica*. The present results clearly indicated *S. fruticosa* and *S. monoica* as potential halophytes with differential photosynthetic and physio-chemical responses for reclamation of saline land through vegetation restoration for biomass production. Further *S. monoica* exhibited superior responses; thus, under increasing atmospheric CO_2 condition, this would be the plant of choice. The study would be helpful in designing the management strategies to combat global climate changes in degraded land through vegetation restoration using halophytes.

Conclusion

S. fruticosa and *S. monoica* are important halophytes, and leaf histology does not differentiate CO_2 fixation mode in these halophytes. The stable isotope ratio supported the operation of C_3 or intermediate CO_2 fixation pathway in *S. fruticosa*. *S. monoica* exhibited better photosynthetic gas exchange and a lower degree of ROS-induced damages under abiotic stress at eCO_2. *S. monoica* under stress exhibited comparatively better photosynthetic pool size, maximum photosynthetic potential of PSII, water splitting, basal quantum yield of non-photochemical processes in PSII, light absorption, heat dissipation, and maximum electron transport flux at both levels of CO_2. Assimilation of C and N supported efficient photosynthetic C-sequestration in *S. monoica* as compared to *S. fruticosa*. Expression analysis of C_4 pathway genes under stress and at eCO_2 suggested their involvement in stress tolerance. Overall, the eCO_2 induced differential responses in these species under stress, and *S. monoica* responded comparatively better due to sufficient availability of photosynthetic assimilates because of its effective C-sequestration potential.

Supplementary Information The online version contains supplementary material available at https://doi.org/10.1007/s00344-021-10485-1.

Acknowledgements CSIR-CSMCRI PRIS—113/2018. The authors are thankful to CSIR (Government of India), New Delhi for establishment of infrastructure facility and GSBTM, Govt. of Gujarat for financial support under GAP2080 (80G2DT) project. The authors also acknowledge the help of ADE&CIF division for SEM, elemental, and ICP analysis. Mr. IH and SAS thank UGC MANF and UGC for Junior/Senior Research Fellowship during their Ph.D. work. The authors are thankful to Dr. D.R. Chaudhary and Prof. Hojeong Kang, School of Civil and Environmental Engineering, Yonsei University, Seoul 03722, South Korea for IRMS analysis. Mr. IH and SAS thank MKSBU, Bhavnagar and AcSIR, Ghaziabad for registration in PhD program, respectively.

Author Contributions Conceptualized and conceived the experiment: MSR/BJ; Designing the experiment: MSR and IH; Experimental execution and Data analysis: IH and SAS; Drafting/editing the manuscript: IH and SAS; Finalization of manuscript: MSR.

Declarations

Conflict of interest Authors declare no conflict of interest.

References

Ahammed GJ, Li Y, Li X, Han WY, Chen S (2018) Epigallocatechin-3-gallate alleviates salinity-retarded seed germination and oxidative stress in tomato. J Plant Growth Regul 37:1349–1356

Ahammed GJ, Li X, Liu A, Chen S (2020a) Brassinosteroids in plant tolerance to abiotic stress. J Plant Growth Regul 39:1451–1464

Ahammed GJ, Li X, Liu A, Chen S (2020b) Physiological and defense responses of tea plants to elevated CO_2: a review. Front Plant Sci 11:305

Ahammed GJ, Li CX, Li X, Liu A, Chen S, Zhou J (2020c) Overexpression of tomato RING E3 ubiquitin ligase gene *SlRING1* confers cadmium tolerance by attenuating cadmium accumulation and oxidative stress. Physiol Plant. https://doi.org/10.1111/ppl.13294

Ainsworth EA, Rogers A (2007) The response of photosynthesis and stomatal conductance to rising (CO_2): mechanisms and environmental interactions. Plant Cell Environ 30:258–270

Ashraf M, Harris P (2004) Potential biochemical indicators of salinity tolerance in plants. Plant Sci 166:3–16

Bates LS, Waldren RP, Teare ID (1973) Rapid determination of free proline for water-stress studies. Plant Soil 39:205–207

Beyer WF Jr., Fridovich I (1987) Assaying for superoxide dismutase activity: some large consequences of minor changes in conditions. Ana Biochem 161:559–566

Bradford MM (1976) A rapid and sensitive method for the quantitation of microgram quantities of protein utilizing the principle of protein-dye binding. Ana Biochem 72:248–254

Bussotti F, Desotgiu R, Cascio C, Pollastrini M, Gravano E, Gerosa G, Manes F (2011) Ozone stress in woody plants assessed with chlorophyll a fluorescence. A critical reassessment of existing data. Environ Exp Bot 73:19–30

Chamovitz D, Sandmann G, Hirschberg J (1993) Molecular and biochemical characterization of herbicide-resistant mutants of cyanobacteria reveals that phytoene desaturation is a rate-limiting step in carotenoid biosynthesis. J Biol Chem 268:17348–17353

Chandler SF, Dodds JH (1983) The effect of phosphate, nitrogen and sucrose on the production of phenolics and solasodine in callus cultures of *Solanum laciniatum*. Plant Cell Rep 2:205–208

Chaudhary DR, Seo J, Kang H, Rathore AP, Jha B (2018) Seasonal variation in natural abundance of δ13C and 15N in *Salicornia brachiata* Roxb. populations from a coastal area of India. Isotopes Environ Health Stud 54:209–224

Cheng G, Wang L, Lan H (2016) Cloning of *PEPC-1* from a C4 halophyte *Suaeda aralocaspica* without Kranz anatomy and its recombinant enzymatic activity in responses to abiotic stresses. Enzyme Microb Technol 83:57–67

Chomczynski P, Sacchi N (1987) Single-step method of RNA isolation by acid guanidinium thiocyanate-phenol-chloroform extraction. Ana Biochem 162:156–159

Demetriou G, Neonaki C, Navakoudis E, Kotzabasis K (2007) Salt stress impact on the molecular structure and function of the photosynthetic apparatus the protective role of polyamines. Biochim Biophys Acta 1767:272–280

Ellsworth DS, Reich PB, Naumburg ES, Koch GW, Kubiske ME, Smith SD (2004) Photosynthesis, carboxylation and leaf nitrogen responses of 16 species to elevated pCO_2 across four free-air CO_2 enrichment experiments in forest, grassland and desert. Global Change Biol 10:121–138

Geissler N, Hussin S, Koyro HW (2009) Interactive effects of NaCl salinity and elevated atmospheric CO_2 concentration on growth, photosynthesis, water relations and chemical composition of the potential cash crop halophyte *Aster tripolium* L. Environ Exp Bot 65:220–231

Geissler N, Hussin S, Koyro HW (2010) Elevated atmospheric CO_2 concentration enhances salinity tolerance in *Aster tripolium* L. Planta 231:583–594

Geissler N, Hussin S, El-Far MM, Koyro HW (2015) Elevated atmospheric CO_2 concentration leads to different salt resistance mechanisms in a C_3 (*Chenopodium quinoa*) and a C_4 (*Atriplex nummularia*) halophyte. Environ Exp Bot 118:67–77

Ghannoum O (2009) C4 photosynthesis and water stress. Ann Bot 103:635–644

Govindjee (1995) Sixty-three years since Kautsky: Chlorophylla fluorescence. Aust J Plant Physiol 22:711–711

Gowik U, Westhoff P (2011) The path from C_3 to C_4 photosynthesis. Plant Physiol 155:56–63

Haque MI, Rathore MS, Gupta H, Jha B (2017) Inorganic solutes contribute more than organic solutes to the osmotic adjustment in *Salicornia brachiata* (Roxb.) under natural saline conditions. Aqu Bot 142:78–86

Havaux M (2014) Carotenoid oxidation products as stress signals in plants. Plant J 79:597–606

Hodges DM, DeLong JM, Forney CF, Prange RK (1999) Improving the thiobarbituric acid-reactive-substances assay for estimating lipid peroxidation in plant tissues containing anthocyanin and other interfering compounds. Planta 207:604–611

Hong Z, Lakkineni K, Zhang Z, Verma DPS (2000) Removal of feedback inhibition of Δ1-pyrroline-5-carboxylate synthetase results in increased proline accumulation and protection of plants from osmotic stress. Plant Physiol 122:1129–1136

Inskeep WP, Bloom PR (1985) Extinction coefficients of chlorophyll a and b in N, N-dimethylformamide and 80% acetone. Plant Physiol 77:483–485

Jacob PT, Siddiqui SA, Rathore MS (2020) Seed germination, seedling growth and seedling development associated physiochemical changes in *Salicornia brachiata* (Roxb.) under salinity and osmotic stress. Aquat Bot 1:166–103272

Jebara S, Jebara M, Limam F, Aouani ME (2005) Changes in ascorbate peroxidase, catalase, guaiacol peroxidase and superoxide dismutase activities in common bean (*Phaseolus vulgaris*) nodules under salt stress. J Plant Physiol 162:929–936

Jin H, Dong D, Yang Q, Zhu D (2016) Salt-responsive transcriptome profiling of *Suaeda glauca* via RNA sequencing. PLoS ONE 11:150504

Keisham M, Mukherjee S, Bhatla SC (2018) Mechanisms of sodium transport in plants progresses and challenges. Int J Mol Sci 19:647

Khatri K, Rathore MS (2019) Photosystem photochemistry, prompt and delayed fluorescence, photosynthetic responses and electron flow in tobacco under drought and salt stress. Photosynthetica 57:61–74

Koteyeva NK, Voznesenskaya EV, Berry JO, Chuong SD, Franceschi VR, Edwards GE (2011) Development of structural and biochemical characteristics of C_4 photosynthesis in two types of Kranz anatomy in genus *Suaeda* (family Chenopodiaceae). J Exp Bot 62:3197–3212

Ksouri R, Megdiche W, Debez A, Falleh H, Grignon C, Abdelly C (2007) Salinity effects on polyphenol content and antioxidant activities in leaves of the halophyte *Cakile maritima*. Plant Physiol Biochem 45:244–249

Kumari J, Udawat P, Dubey AK, Haque MI, Rathore MS, Jha B (2017) Overexpression of SbSI-1, a nuclear protein from *Salicornia brachiata* (Roxb.) confers drought and salt tolerance in tobacco by curtailing oxidative damage and maintaining photosynthetic efficiency. Front Plant Sci 8:1215

Li T, Tao Q, Liang C, Yang X (2014) Elevated CO_2 concentration increase the mobility of Cd and Zn in the rhizosphere of hyperaccumulator *Sedum alfredii*. Environ Sci Pollut Res 21:5899–5908

Li P, Li B, Seneweera S, Zong Y, Li FY, Han Y, Hao X (2019) Photosynthesis and yield response to elevated CO_2, C_4 plant foxtail millet behaves similarly to C_3 species. Plant Sci 285:239–247

Livak KJ, Schmittgen TD (2001) Analysis of relative gene expression data using real-time quantitative PCR and the 2− ΔΔCT method. Methods 25:402–408

Lokhande VH, Srivastava AK, Srivastava S, Nikam TD, Suprasanna P (2011) Regulated alterations in redox and energetic status are the key mediators of salinity tolerance in the halophyte *Sesuvium portulacastrum* (L.) L. Plant Growth Regul 65:287

Long SP, Ainsworth EA, Rogers A, Ort DR (2004) Rising atmospheric carbon dioxide: plants FACE the future. Annu Rev Plant Biol 55:591–628

Mathur S, Mehta P, Jajoo A (2013) Effects of dual stress (high salt and high temperature) on the photochemical efficiency of wheat leaves (*Triticum aestivum*). Physiol Mol Biol Plants 19:179–188

Mehta P, Allakhverdiev SI, Jajoo A (2010) Characterization of photosystem II heterogeneity in response to high salt stress in wheat leaves (*Triticum aestivum*). Photosynth Res 105:249–255

Misra AN, Srivastava A, Strasser RJ (2001) Utilization of fast chlorophyll *a*fluorescence technique in assessing the salt/ion sensitivity of mung bean and Brassica seedlings. J Plant Physiol 158:1173–1181

Miyagawa Y, Tamoi M, Shigeoka S (2000) Evaluation of the defense system in chloroplasts to photooxidative stress caused by paraquat using transgenic tobacco plants expressing catalase from *Escherichia coli*. Plant Cell Physiol 41:311–320

Moghaieb RE, Saneoka H, Fujita K (2004) Effect of salinity on osmotic adjustment, glycinebetaine accumulation and the betaine aldehyde dehydrogenase gene expression in two halophytic plants *Salicornia Europaea* and *Suaeda Maritima*. Plant Sci 166:1345–1349

Morgan JA, LeCain DR, Pendall E, Blumenthal DM, Kimball BA, Carrillo Y, Williams DG, Heisler-White J, Dijkstra FA, West M (2011) C_4 grasses prosper as carbon dioxide eliminates desiccation in warmed semi-arid grassland. Nature 476:202

Oukarroum A, Bussotti F, Goltsev V, Kalaji HM (2015) Correlation between reactive oxygen species production and photochemistry of photosystems I and II in *Lemna gibba* L. plants under salt stress. Environ Exp Bot 109:80–88

Pan C, Ahammed GJ, Li X, Shi K (2018) Elevated CO_2 improves photosynthesis under high temperature by attenuating the functional limitations to energy fluxes, electron transport and redox homeostasis in tomato leaves. Front Plant Sci 9:1739

Park J, Okita TW, Edwards GE (2009) Salt tolerant mechanisms in single-cell C4 species *Bienertia sinuspersici* and *Suaeda aralocaspica* (Chenopodiaceae). Plant Sci 176:616–626

Patterson BD, Payne LA, Chen YZ, Graham D (1984) An inhibitor of catalase induced by cold in chilling-sensitive plants. Plant Physiol 76:1014–1018

Pérez-Romero JA, Idaszkin YL, Barcia-Piedras JM, Duarte B, Redondo-Gómez S, Caçador I, Mateos-Naranjo E (2018) Disentangling the effect of atmospheric CO_2 enrichment on the halophyte *Salicornia ramosissima* J. Woods physiological performance under optimal and suboptimal saline conditions. Plant Physiol Biochem 127:617–629

Ranjbarfordoei A, Samson R, Van DP (2006) Chlorophyll fluorescence performance of sweet almond [*Prunus dulcis* (Miller) D. Webb] in response to salinity stress induced by NaCl. Photosynthetica 44:513–522

Rathore AP, Chaudhary DR, Jha B (2016) Biomass production, nutrient cycling, and carbon fixation by *Salicornia brachiata* Roxb.: A promising halophyte for coastal saline soil rehabilitation. Int J Phytoremediation 18:801–811

Rathore MS, Balar N, Jha B (2019) Population structure and developmental stages associated eco-physiological responses in *Salicornia brachiata*. Ecol Res 34:644–658

Rondeau P, Rouch C, Besnard G (2005) NADP-malate dehydrogenase gene evolution in Andropogoneae (Poaceae): gene duplication followed by sub-functionalization. Ann Bot 96:1307–1314

Rozema J, Dorel F, Janissen R, Lenssen G, Broekman R, Arp W, Drake BG (1991) Effect of elevated atmospheric CO_2 on growth, photosynthesis and water relations of salt marsh grass species. Aqu Bot 39:45–55

Sage RF (2004) The evolution of C4 photosynthesis. New Phytol 161:341–370

Sage RF, Coleman JR (2001) Effects of low atmospheric CO_2 on plants: more than a thing of the past. Trends Plant Sci 6:1360–1385

Salvatori E, Fusaro L, Gottardini E, Pollastrini M, Goltsev V, Strasser RJ, Bussotti F (2014) Plant stress analysis: application of prompt, delayed chlorophyll fluorescence and 820 nm modulated reflectance. Insights from independent experiments. Plant Physiol Biochem 85:105–113

Schansker G, Tóth SZ, Strasser RJ (2005) Methylviologen and dibromothymoquinone treatments of pea leaves reveal the role of photosystem I in the Chl a fluorescence rise OJIP. BBA-Bioenergetics 1706:250–261

Schwarz M, Gale J (1983) The effect of heat and salinity stress on the carbon balance of *Xanthium strumarium*. Effects of stress on photosynthesis. Springer, Dordrecht, pp 325–333

Shomer-Ilan A, Beer S, Waisel Y (1975) *Suaeda monoica*, a C_4 plant without typical bundle sheaths. Plant Physiol 56:676–679

Singh A, Agrawal M (2015) Effects of ambient and elevated CO_2 on growth, chlorophyll fluorescence, photosynthetic pigments, antioxidants, and secondary metabolites of *Catharanthus roseus* (L.) G Don. grown under three different soil N levels. Environ Sci Pollut Res 22:3936–3946

Song J, Feng G, Tian CY, Zhang FS (2006) Osmotic adjustment traits of *Suaeda physophora*, *Haloxylon ammodendron* and *Haloxylon persicum* in field or controlled conditions. Plant Sci 170:113–119

Stutz SS, Edwards GE, Cousins AB (2014) Single-cell C_4 photosynthesis: efficiency and acclimation of *Bienertia sinuspersici* to growth under low light. New Phytol 202:220–232

Ueno O, Kawano Y, Wakayama M, Takeda T (2006) Leaf vascular systems in C_3 and C_4 grasses: a two-dimensional analysis. Ann Bot 97:611–621

Voznesenskaya EV, Franceschi VR, Kiirats O, Artyusheva EG, Freitag H, Edwards GE (2002) Proof of C_4 photosynthesis without Kranz anatomy in *Bienertia cycloptera* (*Chenopodiaceae*). Plant J 31:649–662

Wheeler MCG, Tronconi MA, Drincovich MF, Andreo CS, Flügge UI, Maurino VG (2005) A comprehensive analysis of the NADP-malic enzyme gene family of *Arabidopsis*. Plant Physiol 139:39–51

Yadav S, Mishra A, Jha B (2018) Elevated CO_2 leads to carbon sequestration by modulating C_4 photosynthesis pathway enzyme (*PPDK*) in *Suaeda monoica* and *S. fruticosa*. J Photochem Photobiol B 178:310–315

Zhang YH, Chen LJ, He JL, Qian LS, Wu LQ, Wang RF (2010) Characteristics of chlorophyll fluorescence and antioxidative system in super-hybrid rice and its parental cultivars under chilling stress. Biol Plant 54:164–168

Zhang Y, Wang Y, Wen W, Shi Z, Gu Q, Ahammed GJ, Cao K, Shah Jahan M, Shu S, Wang J, Sun J (2020a) Hydrogen peroxide mediates spermidine-induced autophagy to alleviate salt stress in cucumber. Autophagy 5:1–5

Zhang Y, Yao Q, Shi Y, Li X, Hou L, Xing G, Ahammed GJ (2020b) Elevated CO_2 improves antioxidant capacity, ion homeostasis, and polyamine metabolism in tomato seedlings under $Ca(NO_3)_2$-induced salt stress. Sci Hortic 273:109644